

2012-01-01

# Evaluating Hydrocarbon Source Rock For Unconventional Shale Oil Play From Seismic And Well Log Data; Kingak Shale, North Slope, Alaska

Sarah Elisabeth Leedberg

University of Texas at El Paso, seleedberg@miners.utep.edu

Follow this and additional works at: [https://digitalcommons.utep.edu/open\\_etd](https://digitalcommons.utep.edu/open_etd)



Part of the [Geology Commons](#), [Geophysics and Seismology Commons](#), and the [Oil, Gas, and Energy Commons](#)

---

## Recommended Citation

Leedberg, Sarah Elisabeth, "Evaluating Hydrocarbon Source Rock For Unconventional Shale Oil Play From Seismic And Well Log Data; Kingak Shale, North Slope, Alaska" (2012). *Open Access Theses & Dissertations*. 2125.  
[https://digitalcommons.utep.edu/open\\_etd/2125](https://digitalcommons.utep.edu/open_etd/2125)

This is brought to you for free and open access by DigitalCommons@UTEP. It has been accepted for inclusion in Open Access Theses & Dissertations by an authorized administrator of DigitalCommons@UTEP. For more information, please contact [lweber@utep.edu](mailto:lweber@utep.edu).

EVALUATING HYDROCARBON SOURCE ROCK FOR UNCONVENTIONAL SHALE OIL  
PLAY FROM SEISMIC AND WELL LOG DATA; KINGAK SHALE, NORTH SLOPE,  
ALASKA

SARAH ELISABETH LEEDBERG

Department of Geological Sciences

APPROVED:

---

Laura F. Serpa, Ph.D., Chair

---

Katherine A. Giles, Ph.D.

---

Eric A. Hagedorn, Ph.D.

---

Benjamin C. Flores, Ph.D.  
Dean of the Graduate School

Copyright ©

by

Sarah E. Leedberg

2012

## **Dedication**

I would like to dedicate this work to my family.

EVALUATING HYDROCARBON SOURCE ROCK FOR  
UNCONVENTIONAL SHALE OIL PLAY FROM SEISMIC AND WELL LOG  
DATA; KINGAK SHALE, NORTH SLOPE, ALASKA

by

SARAH ELISABETH LEEDBERG, B.A.

THESIS

Presented to the Faculty of the Graduate School of

The University of Texas at El Paso

in Partial Fulfillment

of the Requirements

for the Degree of

MASTER OF SCIENCE

Department of Geological Sciences

THE UNIVERSITY OF TEXAS AT EL PASO

December 2012

## **Acknowledgements**

I would like to thank the following individuals without whom I could not have completed this work. To everyone at the University of Southern Maine especially: Steven Pollock, Charles Fitts, Mark Swanson, Margaret Vose, Karen Glidden, Robert Sanford, Lauren Redmond, and my undergraduate adviser Irwin Novak. Thanks for getting me through the first part of this journey and believing in me. To Jennifer Nocerino and Bob Stewart, the two of you were such a fundamental part of me coming to UTEP; I will never be able to thank you enough. For pushing me in the direction to do this work, I would like to thank Matthew Silverman of Robert L. Bayless, Producer LLC, you were right; this is what needed to be done. Also from Robert L. Bayless, Producer LLC, Cat Campbell, your feedback early on helped to clarify so many issues. Bunmi Elebiju and Pierre-Andre Depret, both from BP, I only wish I could have incorporated more of your ideas. Chima Nzewunwah from Chesapeake Energy Corporation; time and again you set me on the right track and pointed me in the direction I needed to go, you will be a friend for life. Thanks to Sandra Ladewig, Palmira Hart, and Tina Carrick for listening as I blew off steam. To Carlos Montoya for helping me to work the bugs out, giving me the space to figure it out on my own, and being a friend when I needed one. To my committee members Kate Giles and Eric Hagedorn, thank you. My thanks go out to so many at the United States Geological Survey. Paul Decker, thank you for being so quick to respond to all my questions. A special thanks to David Houseknecht for your revisions, for connecting me to so much data, for understanding the scope of what I wanted to accomplish, and for being my go to expert on the Kingak. To Laura Serpa, my adviser, for believing in the idea and making sure I got it done on time. You have been one of my biggest cheerleaders and every time you sang my praises to the world it pushed me on. You understood my limitations and accepted the challenge anyway.

Come see me at retirement time, I believe there was some sort of agreement and I owe you. To my daughter Lucy and my son Ethan, you are both too young to know what you have sacrificed. I promise to make it up to you. Grace, my eldest child, if anyone deserves my gratitude it is you. You have felt this sacrifice perhaps the most. You have not only put up with my dreams coming first, but you were willing to move across the country, twice. You, my angel, will be my priority, along with your brother and sister from this point forward. Finally, the love of my life, my husband; when I asked if I might shake up our world you said yes. You never doubted if I could do this. When I was so tired and wanted to give up you took on more. You let me cry and laughed when I was being crazy. You made all of this possible. I am blessed to know you and I am in awe of you as a father and a husband. Now it is your turn. And, yes, I do believe in you too.

## **Abstract**

It has been proposed that Acoustic impedance (AI) responses can be used to estimate total organic carbon (TOC) within thick, clay rich shale. The purpose of this work is to evaluate the effectiveness of the AI inversion technique, and establish a methodology that can be applied to other basins. The Kingak Formation (lower Jurassic to early Cretaceous), located on the North Slope of Alaska, has been extensively evaluated for its unconventional potential. The Kingak is shale and is known to have greater than 30 percent clay. Because clay has ductile properties it makes it difficult to stimulate a well through hydraulic fracturing. This AI inversion technique was tested by utilizing synthetic seismograms to create an AI curve generated using The KINGDOM Software©. The synthetic seismograms were used to ensure a well log to seismic match. The synthetic seismograms also created an AI curve along the well. From these synthetic seismograms the AI value was compared to TOC values. It was from this comparison that a trend was observed that did not match the predicted trend. I believe the discrepancy observed was due to the sampling method. Based on this observation, I conclude that the method of tracking TOC with AI responses requires extremely controlled sampling methods; therefore it is not a beneficial method of revisiting old data sets in hopes of identifying new prospects.



## Table of Contents

Acknowledgements .....	v
Abstract .....	vii
Table of Contents .....	viii
List of Tables .....	xi
List of Figures .....	xii
Introduction .....	1
Background.....	2
TOC (Total Organic Carbon).....	2
AI (Acoustic Impedance).....	4
North Slope .....	4
Kingak Shale .....	7
Evaluation of TOC levels on Seismic with AI Signatures .....	11
Methods .....	14
Well Logs.....	15
Synthetic Seismograms.....	16
Plots... ..	17

Data .....	17
Wells .....	17
Sample intervals .....	18
Sample types .....	18
Seismic .....	18
Analysis .....	19
Plots.. .....	19
Seismic relationship .....	21

Results .....	23
Future Work.....	26
Summary.....	26
Work Cited.....	27
Appendix .....	29
A: Sample Style.....	29
B: Ikpihpuk.....	30-36
C: Inigok.....	37-43
D: N Inigok.....	44-49
E: W Kuparuk.....	50-56
F: Structural Map North Slope.....	57
G: N-PR-81-AK.....	58
H: W-40-80-AK.....	59
I: Alternate Trend lines.....	60-61
J: Single Point Alternate Trend lines.....	62
Vita.....	63

## List of Tables

Table 1: Well metadata.....	13
-----------------------------	----

## List of Figures

Figure 1: HI vs. OI .....	2
Figure 2: Rock Eval Pyrolysis. ....	3
Figure 3: North Slope Oil Fields.....	6
Figure 4: Generalized Stratigraphy, North Slope .....	7
Figure 5: Sequence Sets Kingak .....	8
Figure 6: Kingak on Seismic .....	10
Figure 7: Well Petrophysics .....	11
Figure 8: Loseth Non-linear Trend. ....	12
Figure 9: Passey TOC Curve .....	12
Figure 10: Loseth TOC Curve on Seismic. ....	13
Figure 11: Loseth Inversions .....	14
Figure 12: Location of Data Set.....	15
Figure 13: Synthetic Seismogram.....	16
Figure 14: Individual Plots.....	19-20
Figure 15: Combined Wells.....	21
Figure 16: TOC Concentration on Seismic N Inigok.....	22
Figure 17: N Inigok Petrophysics.....	23

## **Introduction**

A shale oil play is an unconventional play because the target of exploitation is the source rock rather than the conventional reservoir rocks. A process called hydraulic fracturing is implemented at the shale formation to create a fracture network allowing hydrocarbons to migrate from a low permeability source rock in to the well. The unconventional play has lower geologic risks than conventional play development; however, the engineering risk is much greater. This is in part due to the fact that shales often have high clay content. As clay has ductile properties, it can make the process of fracturing the rock less effective. Therefore when a potential source rock target has been identified the amount of clay must be weighed against the overall potential of the source rock. One way of gauging the potential of the source rock is a thorough understanding of the total organic carbon (TOC) that is trapped within the source rock. The Kingak shale on the North Slope of Alaska, is clay rich but with high overall TOC. Because developing unconventional plays can significantly extend recoverable oil reserves targeting the areas within the shale with the highest concentrations of TOC will mitigate some of the engineering risk. Løseth et al. [2011] suggest a method for determining the amount of TOC in a shale by evaluating well logs and seismic reflection data; specifically with regard to their acoustic impedance (AI) responses. I applied this technique to the Kingak Shale to determine where the most promising hydrocarbon rich targets are located within the formation.

Løseth et al. [2011] documented a nonlinear correlation between AI and TOC within shale that has high (>30%) clay content. Specifically, as the AI decreased the TOC should increase relative to the nonlinear curve. The Kingak is a clay-rich shale so it is expected to show the variations described by Løseth et al. [2011] but instead the results of my study were just the opposite. I observed a linear increase of the TOC with increasing AI. The data set I used included samples from the Kingak formation that was processed at several different labs and at

varying depth intervals within the formation ranging from a single point to greater than 70 meters. The method of sampling was also inconsistent and included cuttings, core samples, drilling mud, and sidewall cores. I believe the reason my results were not consistent with those predicted by Løseth et al. [2011] is not necessarily a failure of the method but is due to the way the formation was sampled.

## Background

### TOC (Total Organic Carbon)

An understanding of what Total Organic Carbon (TOC) is and the role it plays in evaluating a source rock for its risk versus its potential. Petroleum is made up of 85% Carbon, 13% Hydrogen, and 2% Oxygen, Sulfur, and Nitrogen. TOC is the weight percent of *organic* carbon in a rock (mg organic carbon/g rock). The weight percent of TOC is determined using a process called *Rock-Eval Pyrolysis* in which a sample of rock is slowly heated to a maximum temperature (T-max: after which the hydrocarbon potential degrades). During this process various spikes are recorded. Kerogen, a heavy organic compound, is insoluble in normal organic solvents such as alcohol and ethanol. Bitumen, a component of kerogen is soluble. Because of this TOC is both movable (bitumen) and immovable (residual, insoluble kerogen). When kerogen is

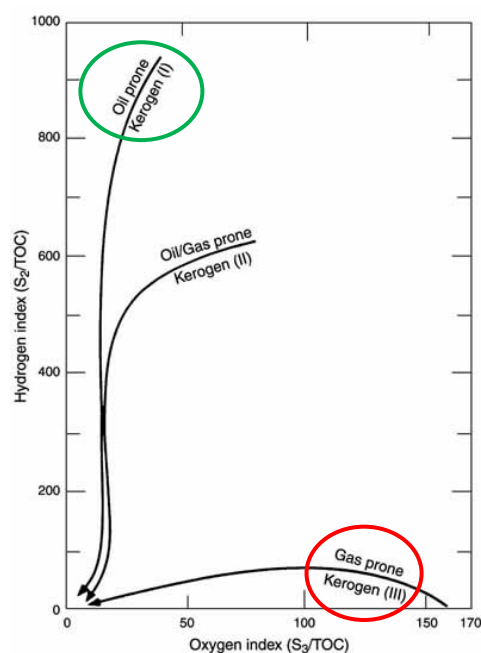


Figure 1: Relationship of Hydrogen and Oxygen to TOC is indicative of what type of Kerogen the source rock is likely to contain. High hydrogen and low oxygen (green) will likely result in oil from the source rock. If there is high oxygen and low hydrogen then the source rock will likely produce gas (red). Modified from TAMU. 2011.

heated for long enough and at the right temperature (60-200 °C) it will “crack” and form hydrocarbons [TAMU, 2011].

Geochemists can replicate what occurs deep within the Earth through the Pyrolysis process. By this process much can be learned about the nature of the organic carbon within a source rock. A sample of the source rock is placed within a vacuum tube in an inert gas. The temperature is slowly increased and as it does a recording device monitors spikes and can

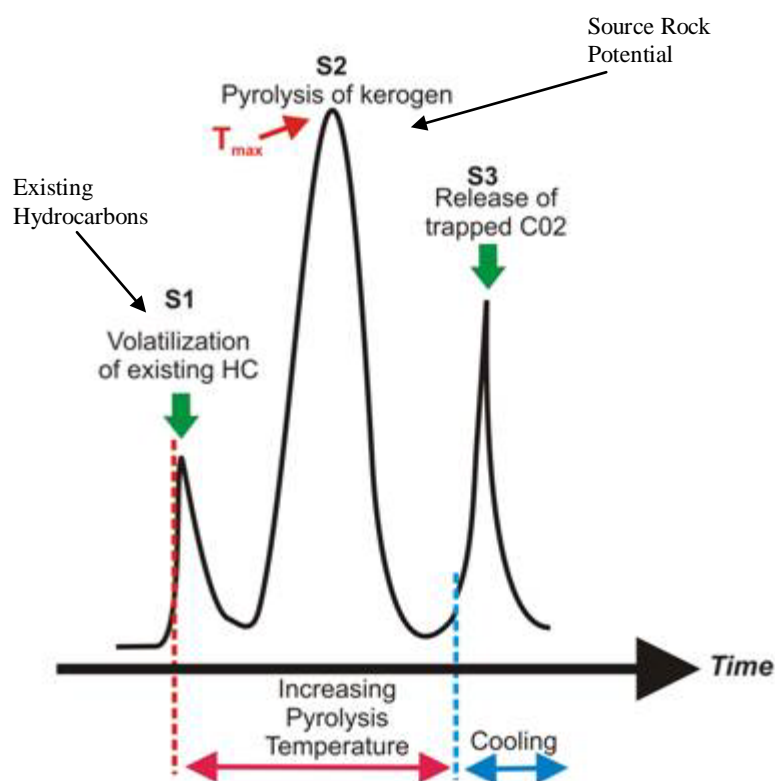


Figure 3: Example of spike sets recorded during *Rock Eval Pyrolysis*. The S1 spike indicates the existing, movable hydrocarbons. The S2 spike indicates the overall source rock potential for producing hydrocarbons as well as the maximum temperature the rock can be exposed to before becoming over mature. S3 indicates the oxygen in the source rock. Modified from [TAMU, 2011].

distinguish the difference between the movable hydrocarbons and the immovable (also known as dead) hydrocarbons. The first spike, S<sub>1</sub>, indicates the amount of free hydrocarbons concentrated in the rock, those that can move. The second spike, S<sub>2</sub>, is the amount of hydrocarbon the rock has the potential to produce under the right conditions (oil and gas window 60-200 °C). The peak of the S<sub>2</sub> spike also represents the temperature at which the maximum hydrocarbon will be



released from the rock. The third spike,  $S_3$ , is the indication of the amount of oxygen in the kerogen. From these spikes the labs are able to calculate the TOC of the source rock. Moveable hydrocarbons are those hydrocarbons that when subjected to sufficient temperature are able to migrate from the source rock. Immoveable hydrocarbons are “dead” kerogen and regardless of temperature will never escape the rock; rather they have been absorbed by the matrix. What petroleum geologists are interested in are the moveable hydrocarbons. That is not to say the hydrocarbons are not often restricted to the source rock due to lack of permeability, but if the permeability were increased they would freely move out of the rock [TAMU, 2011].

### **AI (Acoustic Impedance)**

Acoustic Impedance (AI) is the product of density and velocity ( $\rho V$ ). It is related to the reflection coefficient (R) where:

$$R = (\rho_2 V_2 - \rho_1 V_1) / (\rho_2 V_2 + \rho_1 V_1) \quad (1.1)$$

and R determines the amplitude, or brightness, observed on seismic image reflections. In this equation  $\rho_1 V_1$  and  $\rho_2 V_2$  represent the change in AI, at a given interface [Ashcroft, 2011].

### **North Slope**

The North Slope is a foreland basin formed during the fold and thrust of the Brooks Range uplift [Handschy, 1998]. The oldest megasequence, the Franklinian, was deposited along a stable continental platform [Mull *et al.*, 1987]. The Franklinian sequence ended at the beginning of the Ellesmerian Orogeny when it was buried, metamorphosed, and deformed [Mull *et al.*, 1987; Handschy, 1998]. The Ellesmerian megasequence was formed during the Ellesmerian Orogeny as uplifted Franklinian rocks were shed from the north (what is now the Beaufort Sea) into the south-facing passive margin of the Arctic Basin [Thomas *et al.*, 2007]. The Beaufortian megasequence began when the counter clockwise rotational rifting of the North

Slope from Arctic Canada created the Arctic Ocean [*Thomas et al.*, 2007]. Much of the Beaufortian sediments were shed from the Barrow Arch, an asymmetric rift shoulder formed in pulses of uplift [*Mull et al.*, 1987]. It was during these pulses that several unconformities were formed and can be observed throughout the North Slope. The most pronounced of these, the Lower Cretaceous Unconformity (LCU), regionally extends from east to west and is truncated along the Barrow Arch to the north (Houseknecht & Bird, 2004) [ *Mull et al.*, 1987; *Peters et al.*, 2006; *Thomas et al.*, 2007]. The Brookian megasequence contains source rock as well as providing necessary over burden for maturation; it was formed during the Brooks Range uplift which culminated in the present day foreland basin [*Handschy*, 1998; *Thomas et al.*, 2007]. It was deposited as a prograding delta from the south to the north [*Peters et al.*, 2006]. (For a structural map of the North Slope of Alaska please refer to Appendix F)

The proven petroleum resources of the North Slope of Alaska are the result of an abundance of source rock [*Thomas et al.*, 2007]. Within three of the four North Slope megasequences: the Brookian, Beaufortian, and Ellesmerian (Figure 4), are found multiple viable source rocks [*Thomas et al.*, 2007]. The Brookian sequence contains several source rocks of which the gamma-ray zone (GRZ) within the Hue Shale and the Pebble Shale units are the most well known [*Mull et al.*, 1987; *Thomas et al.*, 2007]. The Beaufortian sequence is comprised solely of the Kingak Shale [*Mull et al.*, 1987; *Houseknecht and Bird*, 2004; *Peters et al.*, 2006].

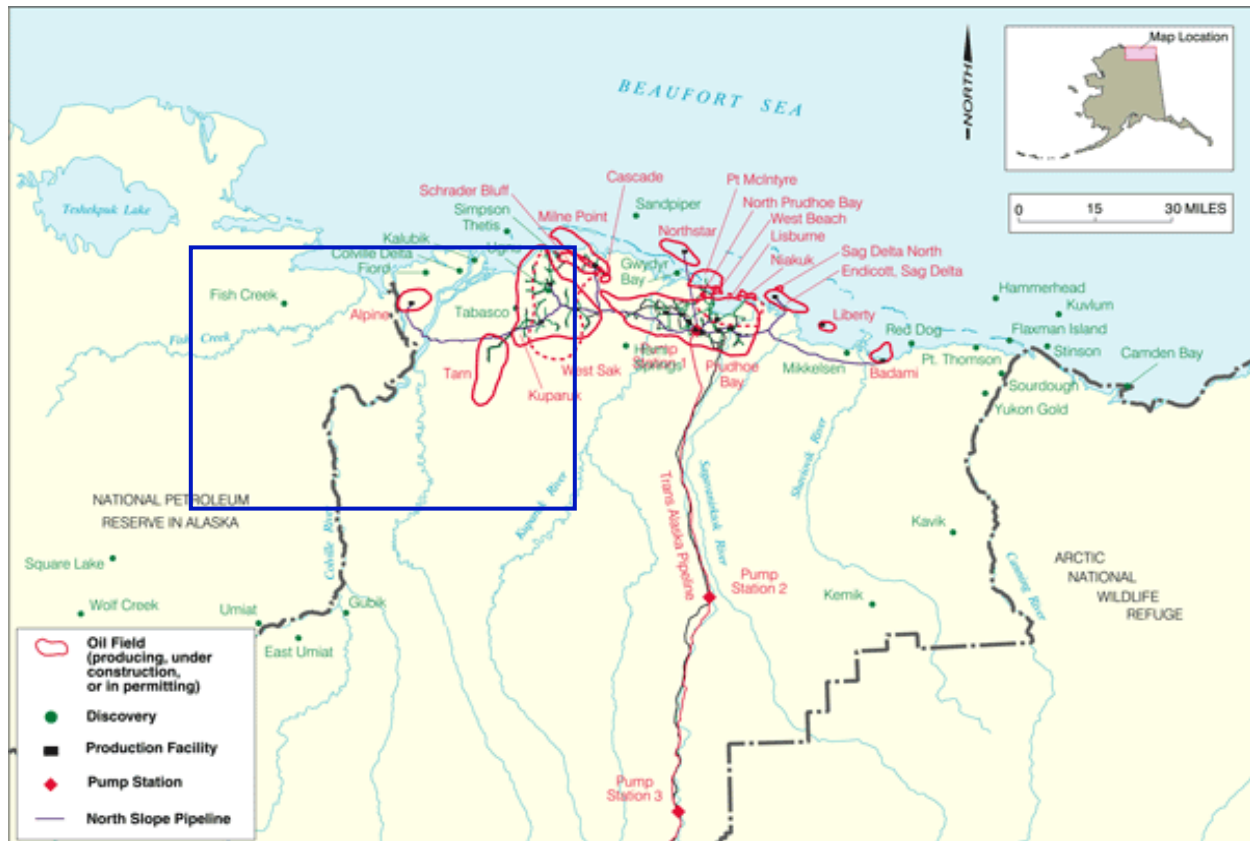


Figure 3: North Slope, Alaska major oil and gas fields. Blue box indicates study area. Modified from <[tapseis.anl.gov/guide/photo/akoilflds.html](http://tapseis.anl.gov/guide/photo/akoilflds.html)> accessed December, 2012

Finally the Ellesmerian sequence contains the Shublik, Kavik, Lisburne, and Kayak shales [Mull *et al.*, 1987; Peters *et al.*, 2006; Thomas *et al.*, 2007].. The Franklinian megasequence is made up of metasedimentary and igneous rocks, and is considered the economic basement and contains no source rock [Mull *et al.*, 1987; Thomas *et al.*, 2007]. It is the Ellesmerian sequence, specifically the Shublik, from which 90% of the oil and 82% of the gas from the North Slope has been generated; the remaining contribution is attributed to the Kingak shale and the Brookian shales [Peters *et al.*, 2006].

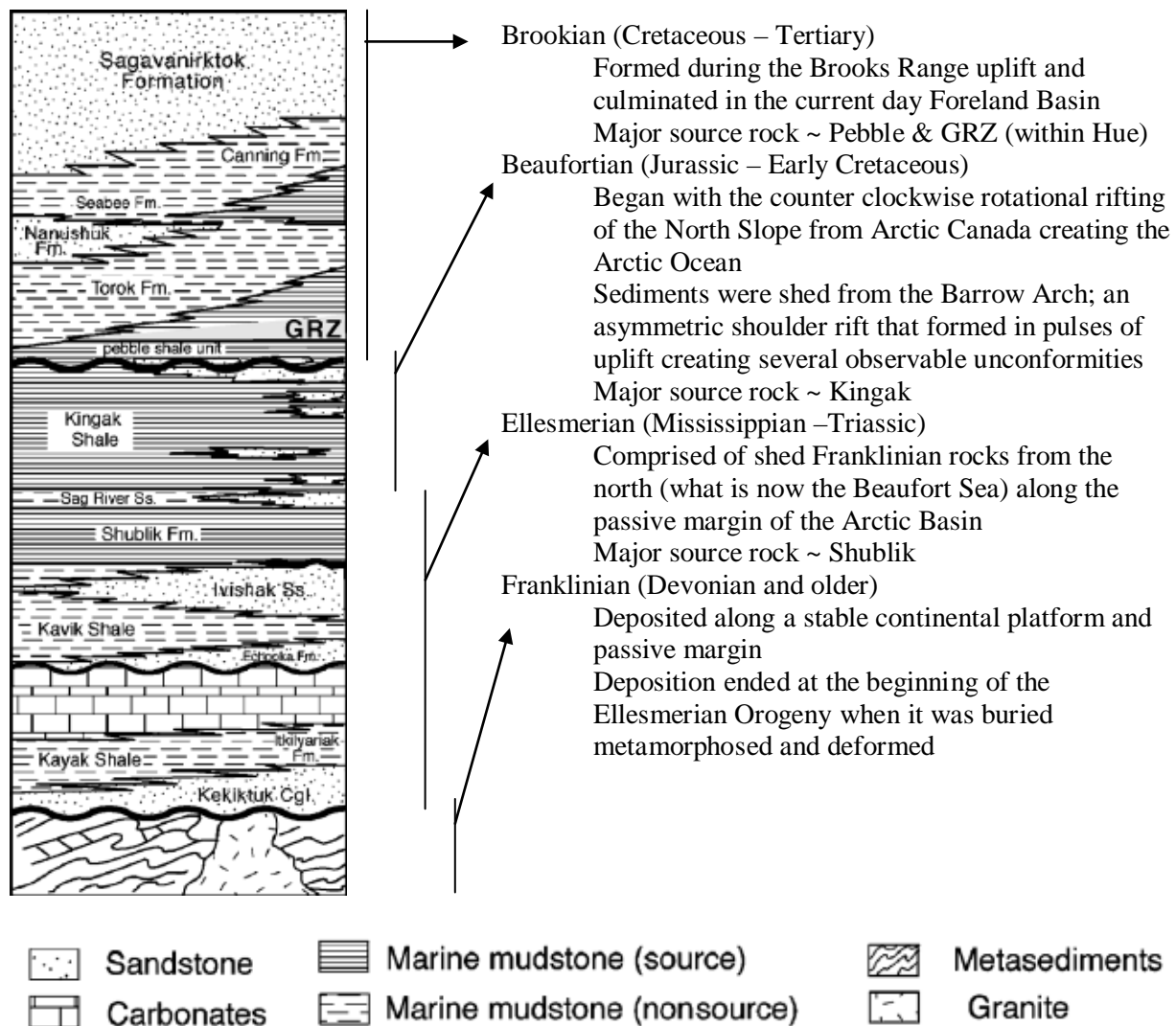


Figure 4. Generalized stratigraphy of the North Slope. Outlined are four Megasequences. The Kingak lies within the Beaufortian Megasequence. Modified from Peters et. al., 2006.

## Kingak Shale

The Kingak Shale is the product of erosion and rifting that occurred as the Arctic Ocean Basin opened roughly 136 million years ago [Houseknecht & Bird, 2004]. It is part of the larger Beaufortian megasequence, and contains of four smaller sequence sets [Houseknecht, 2001].

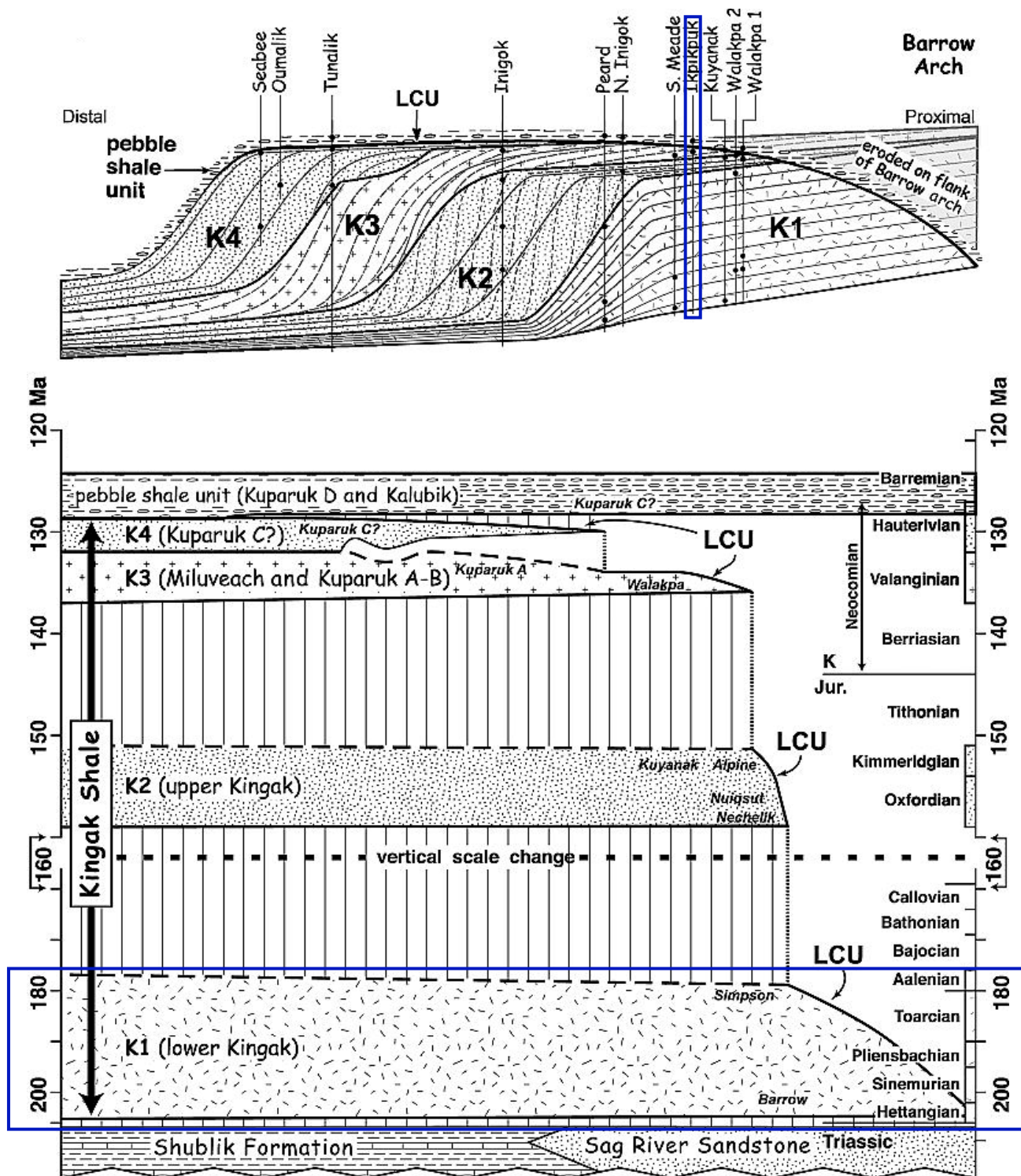


Figure 5: Four sequence sets of the Kingak formation. Blue boxes indicate the seismic section shown in Figure 6 with the minor sequence sets mapped from the Gamma Ray log. Three of the wells selected for this study are included in the above image: Ikpikpuq, Inigok, and N Inigok. From the Ikpikpuq well I was able to identify the minor sequences within the K1 sequence set. From the Inigok well I was able to identify the minor sequences within the K2 sequence set. Modified from Houseknecht & Bird, 2004.

Each set is made up of multiple transgressive-regressive minor sequences [*Houseknecht and Bird, 2004*]. The earliest sequence (K1) contains condensed shales, and is the best candidate for the contributor to the oil fields of the North Slope [*Peters et al., 2006*]. The minor sequences sets [*Houseknecht & Bird, 2004*] of the K1 and K2 units were identified using the Gamma Ray from the well log and were successfully correlated to seismic (Figure 6 for K1 minor sequence set correlation to seismic). The thickest portion (~1200 m) of the Kingak shale is found in the southwest portion of the National Petroleum Reserve Alaska NPRA [*Houseknecht & Bird, 2004*]. The Kingak thins northward towards the Barrow Arch and is ultimately truncated by the Lower Cretaceous Unconformity [*Handschy, 1998; Houseknecht & Bird, 2004*]. This was aided by the fact that clay stone with low-density organic matter has a characteristic strong negative reflection at the top of the source rock and a corresponding positive reflection at the base of the source rock [*Løseth et al., 2011*]. The Kingak has an average TOC of 5% and clay content of greater than 30% [*Houseknecht et. al., 2012*].

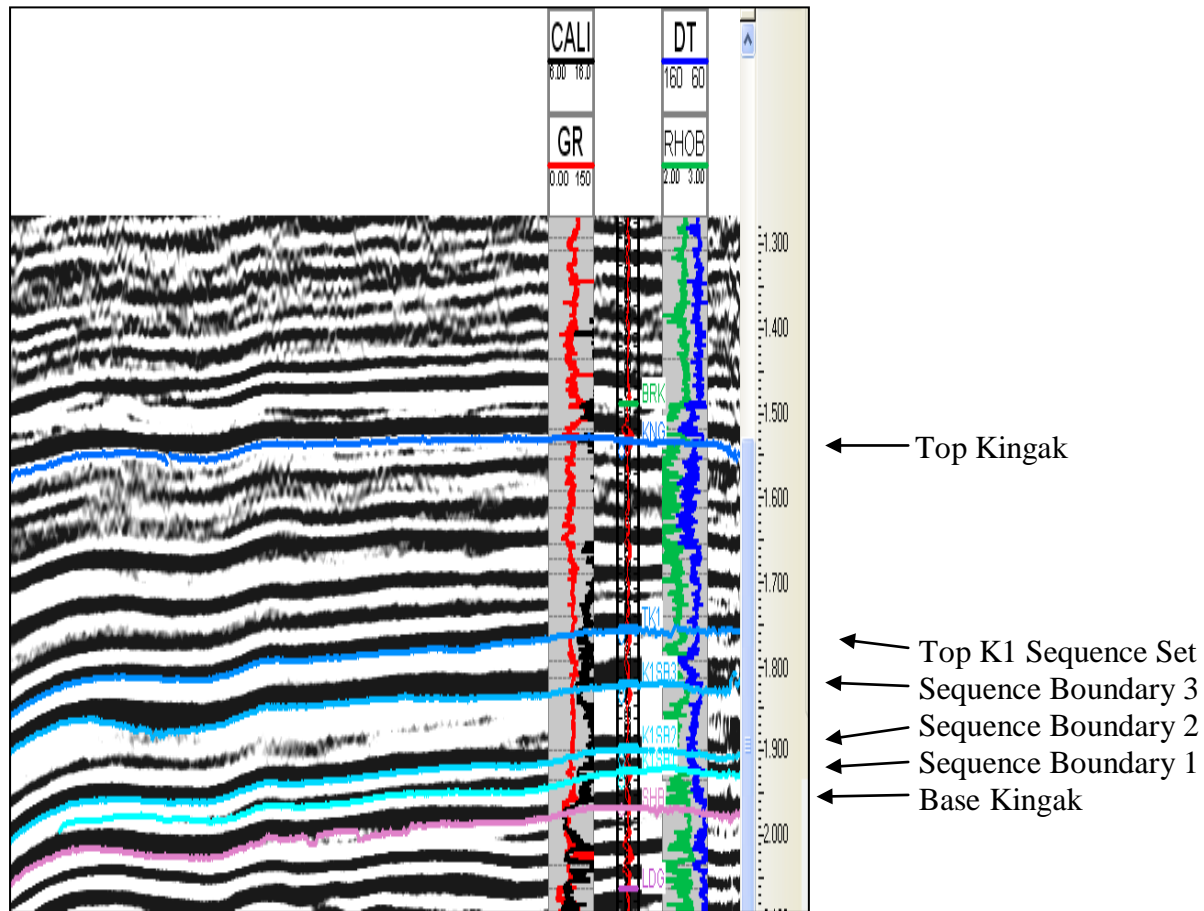


Figure 6: Seismic section along line 22-81 showing the Kingak formation. Well log curves are from the Ikpihpuk well. Red log curve is the Gamma Ray from which the blue lines mapping the minor K1 sequence boundaries were identified as proposed by Houseknecht and Bird, 2004.

Based on evidence from analogue fields, such as the Alpine field [Bailey, 2010], as well as petrophysical analysis from well data, it is evident that the oil has migrated from the older sequence sets into the younger as indicated in orange along the Ikpihpuk and W Kupaupuk wells (Figure 7) petrophysical analysis. The oil has also migrated from deeper in the basin up dip towards the Barrow Arch as seen along the West Kupaupuk St 3-11-11 well.



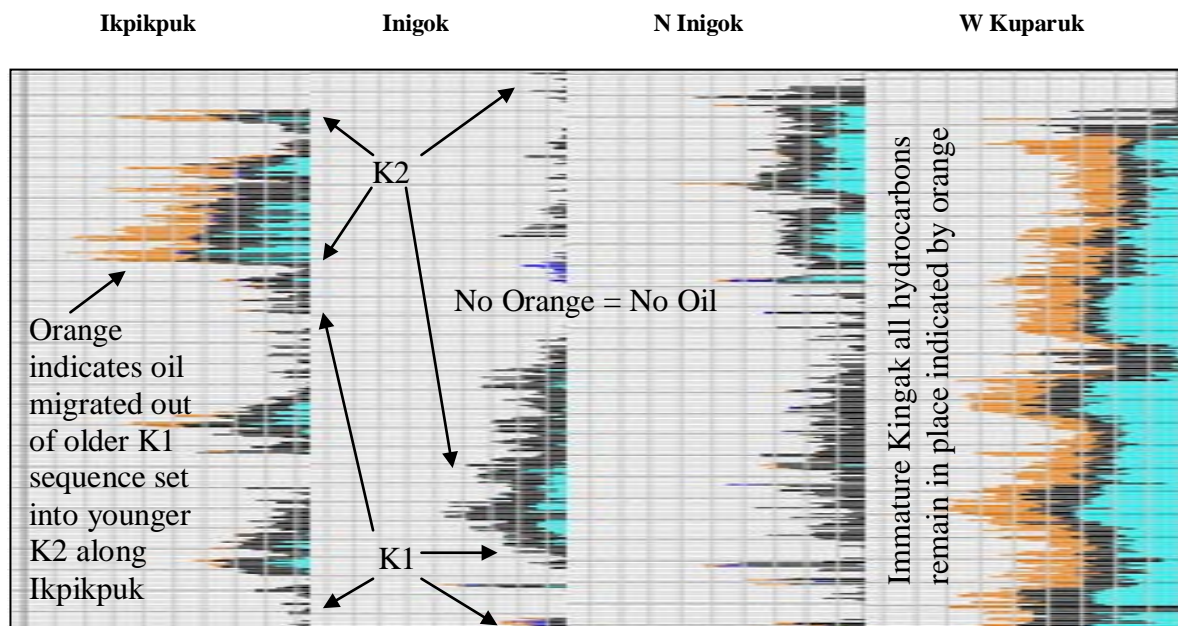


Figure 7: Petrophysical analysis of the Kingak Shale. Orange indicates hydrocarbons that remain in place (unmigrated). Teal indicates water saturation. Images are from each of the four wells left to right: Ikpikpuk (mature and has remaining hydrocarbons), Inigok (spent, no extractable hydrocarbons remain), N Inigok (spent, no extractable hydrocarbons remain), and W Kugaruk (immature, the source rock itself has not reached sufficient temperature to “crack”). The Ikpikpuk is located on the western margin of the Umiat Basin, while the W Kugaruk is along the northeastern margin. Both Inigok and N Inigok are found within the deepest part of the Umiat Basin.

An X-Ray Diffraction report found on the State of Alaska Department of Natural Resources web site indicates that the most common clays in the Kingak shale are moderate amounts of illite/smectite mixed layer clay (15%), major amounts of illite, in some cases >35%, and moderate amounts of chlorite and kaolinite ranging from 13-35% [State of Alaska Department of Natural Resources: Alaska Geologic Materials Center, 2009].

### Evaluation of TOC levels on Seismic with AI Signatures

Løseth et al., [2011] established that for a low-density organic-rich clay stone it was possible to invert seismic data to highlight TOC bright spots. The study included a three step method of determining where the TOC was most concentrated in a formation.



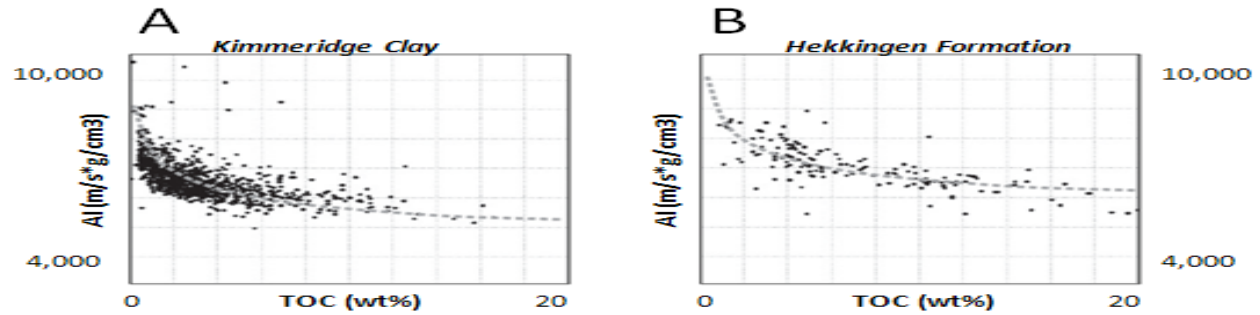


Figure 8: Results of non-linear trend. Plot A from Metherrhills Quarry well in Kimmeridge Clay core samples. Plot B from Hekkingen Formation, Barents Sea, 9 wells using cuttings. Modified from Løseth et al., [2011].

The first step was in establishing the correct non-linear relationship between AI and TOC. For this purpose they selected marine source rock clay stones: Draupne (North Sea), Spekk (Norwegian Sea), Hekkingen (Barents Sea), and Kimmeridge Clay (England). Using core samples from a single well in the Kimmeridge Clay source rock and cuttings from 9 wells in the Hekkingen Formation they plotted the TOC values with corresponding AI values (Figure #). The non-linear trend was similar at both locations and a baseline curve was established. No equation was given for the curve nor was there any method noted for establishing the curve.

The second step followed the establishment of the baseline curve. During this step they used the log data (resistivity and sonic) as proposed by Passey et al. [1990] to create a pseudo log for the TOC. In this method the logs are overlain and the difference between the two logs is then plotted as a TOC curve. The theoretical TOC log curve is then smoothed and applied along the corresponding seismic line. It was from there that they observed the seismic lines had very different amplitude responses depending on where the TOC was concentrated in the shale (Figure 10).

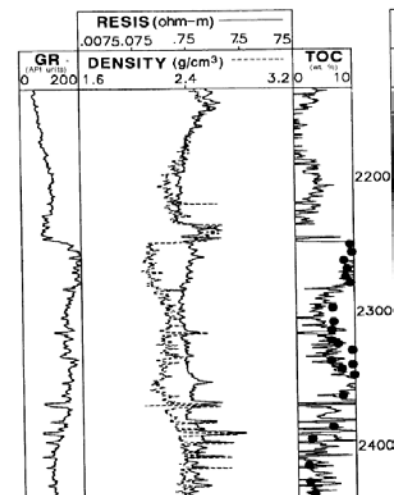


Figure 9: Sample of TOC profile created using Passey et. al. method [1990]. Modified from Passey et. al., [1990]

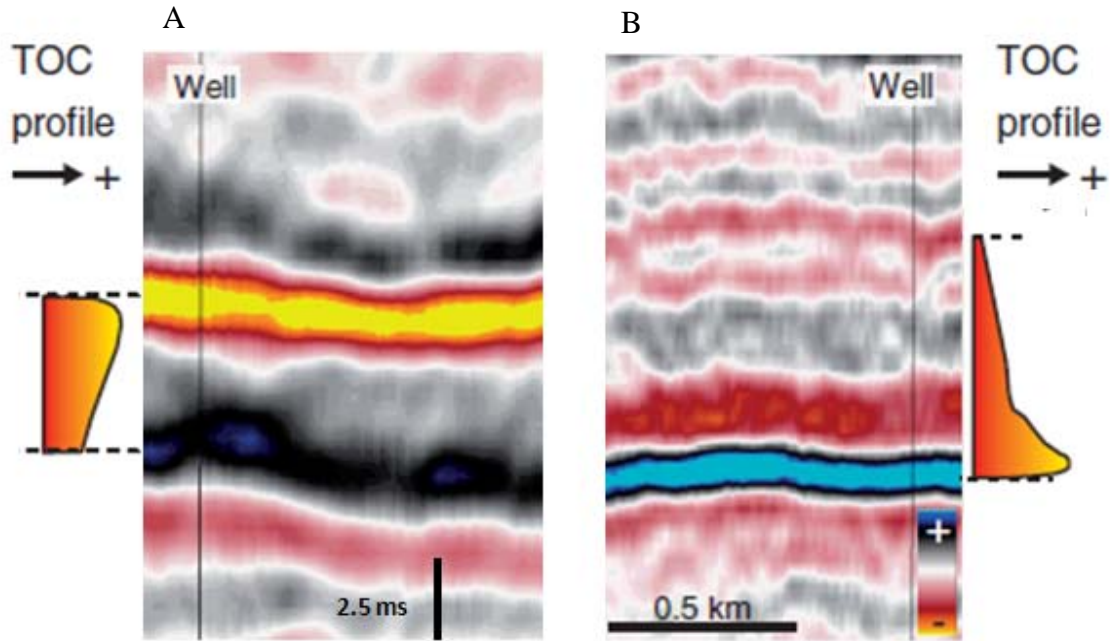


Figure 10: A: TOC curve indicates upward increase with the top negative reflector being the strongest of the two. B: TOC curve indicates that the TOC is most concentrated at the base of the source rock and has the stronger positive base reflection with very weak top reflection. Dashed lines indicate top and base of source rock. Modified from *Løseth, et al., 2011*.

If the TOC increased upward in the shale (Figure 10A) then the strongest reflection would be found at the top of the shale. Likewise if the TOC was concentrated at the base of the shale (Figure 10B) then the bottom reflector would be the most pronounced.

Finally once the non-linear relationship (baseline curve) had been established, and the TOC curve created and matched to seismic, two separate inversions were implemented. The first inversion was from seismic to an AI profile. The amplitudes along the seismic lines were inverted to equivalent AI responses. This is possible because the R represents the amplitude observed on seismic images. In equation 1.1,  $\rho_2 V_2 - \rho_1 V_1$  represents the change in AI,  $(\rho V)$ , at a given interface. It is because of this direct relationship that the seismic amplitudes can be inverted to the AI. The second inversion took the created AI profile and inverted it to match the

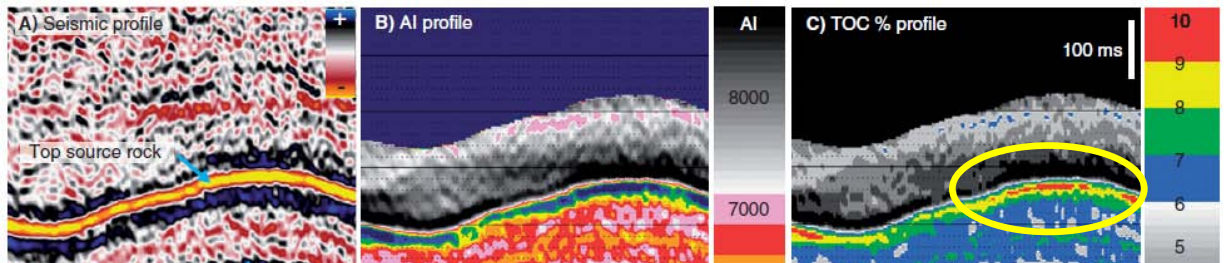


Figure 11: Converting seismic to a TOC profile is a two step inversion. First the seismic is inverted to an AI profile. Next the AI profile is inverted to the TOC profile assumed to have been established for the formation using the baseline curve. Yellow circle indicates the highest zone of TOC concentration. Modified from Løseth, et al., 2011

TOC baseline curve that had been generated in the original relationship. The result was a clearly defined bright spot highlighting the most concentrated area of TOC within the shale.

## Methods

This study focuses on the North Slope's Kingak Shale, which is clay-rich [Houseknecht et al., 2012] and therefore poses a significant engineering risk due to the unpredictable nature of clay in response to hydraulic fracturing. I compiled AI signatures with their respective TOC values by utilizing synthetic seismograms (Figure 13 and Appendixes B-E) created using the KINGDOM© Software. Well data were uploaded from the Alaska Department of Natural Resources, Division of Oil and Gas, website [State of Alaska, 2011], and from the U S Department of the Interior USGS online publications directory [US Department of the Interior,

2011]. Seismic data was uploaded to KINGDOM© from the National Archive of Marine Seismic Surveys - USGS PCMSC [USGS, 1974-1981].

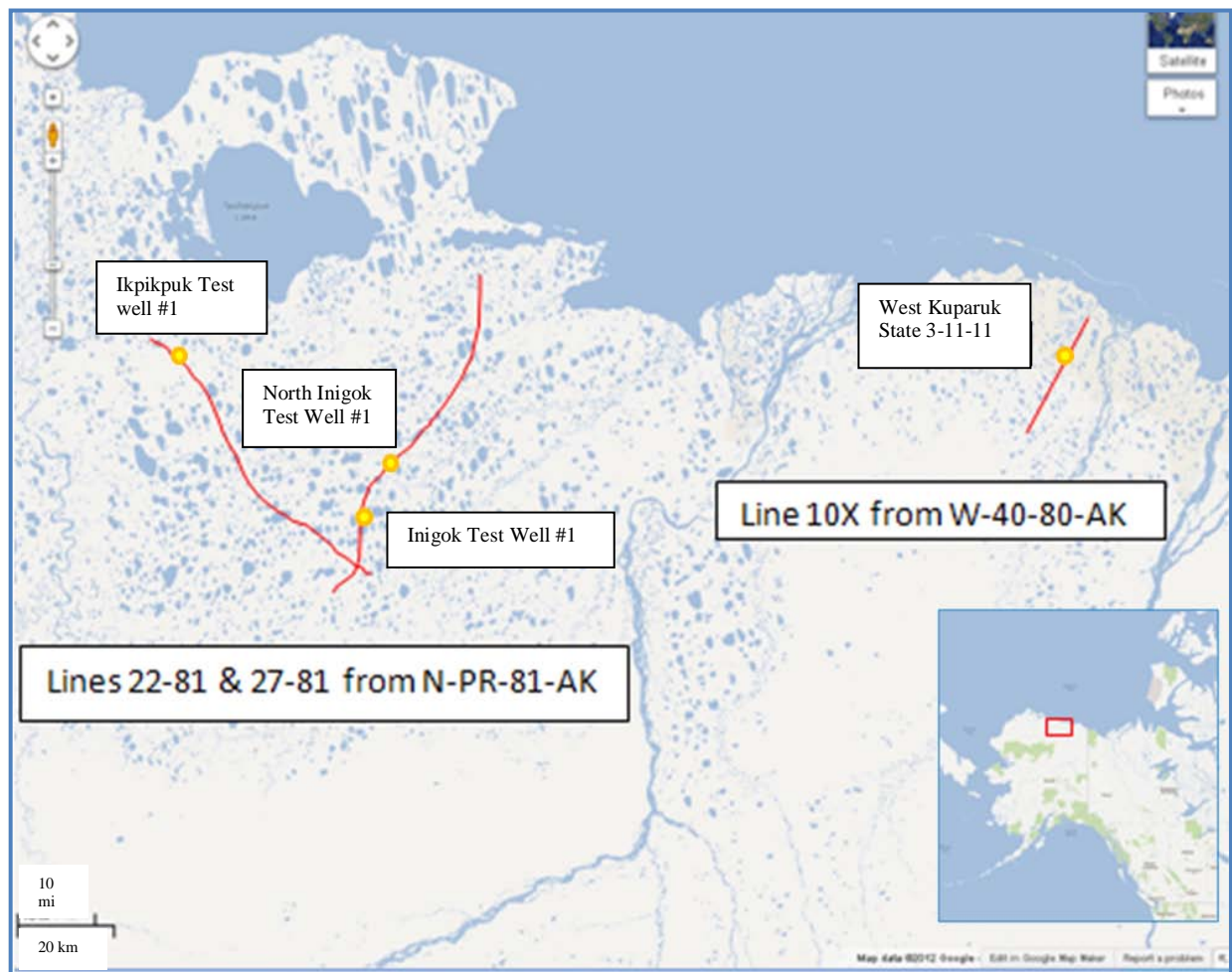


Figure 12: In-set showing location of study area along the North Slope of Alaska. Red lines indicate the approximate location of seismic lines. Yellow circles indicate approximate location of wells. Image modified from Google Maps.

## Well Logs

Four wells were selected: Ikpikuk #1, Inigok #1, N Inigok #1, and W Kuparuk St 3-11-11. These wells were selected for their varying levels of TOC: mature, spent (both Inigok and N Inigok are economically depleted), and immature respectively [Peters *et al.*, 2006]. The purpose of selecting the different wells at different levels of maturity was to determine if maturity had any bearing on the results.

## Synthetic Seismograms

The synthetic seismograms generated using KINGDOM© produced AI curves along the well therefore facilitating observation of AI at respective depths. Because AI is the product of P-wave velocity and density and the sonic log can be converted to velocity it can then be applied to the density log thus creating a pseudo log for AI.

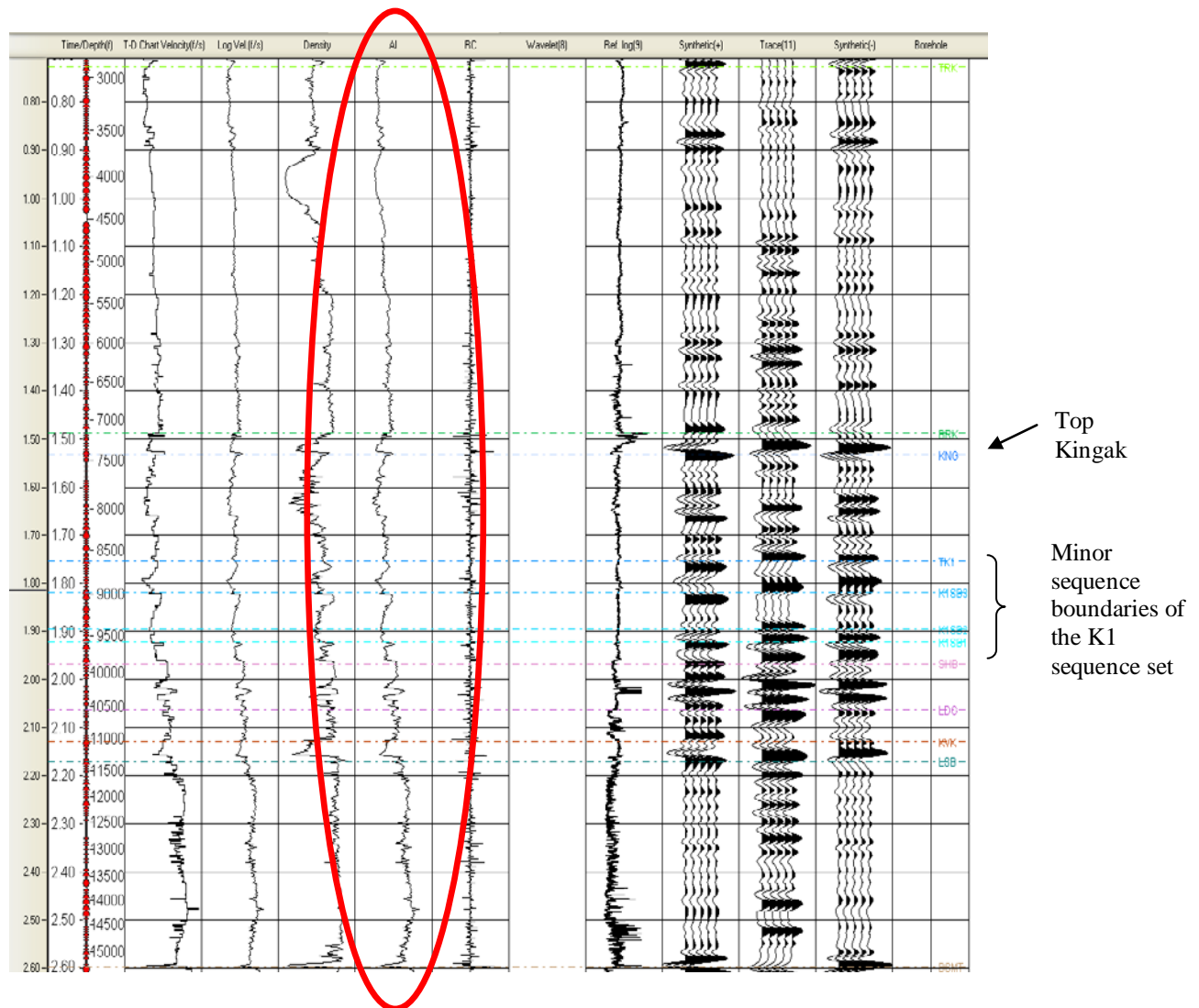


Figure 13: Synthetic Seismogram generated in KINGDOM© using the well data from the Ikpiuk well. The extracted trace (Trace[11] column) is a good match to the synthetic trace generation (Synthetic[-] column). The Ref. log(9) is the gamma ray from which the minor sequence boundaries were identified. Blue-Teal lines all represent the Kingak. Other colored lines represent tops for other formations.



## Plots

Once the synthetic seismogram matched the actual seismic position the AI was entered into the spreadsheet at the appropriate depth. Using Microsoft Excel © spreadsheets were prepared for each of the wells in which the TOC was recorded along with its corresponding depth; the AI for each of those depths was then also recorded. The TOC data were obtained from the USGS Digital Data Series DDS-59 Microsoft Access © database provided by the United State Geological Survey.

## Data

### Wells

Table 1: Metadata

Well	ID	Drilling Season	Operator	Kelly Bushing	Start Depth	End Depth
Ikpikpuk Test Well No. 1	50279200040000	1979-1980	Husky Oil NPR Operations, Inc.	16m	25m	4694m
Inigok Test Well No. 1	50279200030000	1978-1979	Husky Oil NPR Operations, Inc.	33m	15m	6127m
North Inigok Test Well No. 1	50103200170000	1980-1981	Husky Oil NPR Operations, Inc.	51m	34m	3100m
W\st Kuparuk State 3-11-11	50029200140000	Unknown	Mobil Oil Corporation	21m	90m	3520m

### Sample Intervals

A sample interval is the length along which a column cuttings from the well has been extracted. The cuttings are collected in a bin and it is from this bin that the sample is drawn. Exact methods of how the sample is drawn depend on the lab that will be doing the evaluation.

Core samples are drawn from a plug of core extracted at a very specific depth. The term “single depth” is used to describe both core and side wall core extractions as they record the TOC for a single depth point rather than an interval.

The Ikpikpuk had a 9m sample interval for the cuttings, while a single depth was given for the core, drilling mud, and side wall core samples. The Inigok had 26 single depth values, 2 sample intervals of 3m, 1 sample interval of 3.4m, and the remaining 53 samples were 9m sample intervals. The N Inigok had 9m sample intervals for all cuttings with the exception of 3 which had 0.3m sample intervals. The W Kubaruk had the most variation in sample intervals; 9 samples had a singular depth value, 3 samples had 9m sample intervals, 2 samples had 12m sample intervals, 2 samples had 18m sample intervals, 1 sample had a 27m sample interval, and 1 sample had a 73m sample interval. Acoustic impedance readings could be taken roughly every 10 ft along the well. (See Appendix A for details). I created a master list of the TOC and corresponding AI for each well.

### **Sample Types**

A total of 212 samples were found in the Kingak: 51 from Ikpikpuk, 82 from Inigok, 44 from N Inigok, and 35 from W Kubaruk. Of the Ikpikpuk samples, 3 were from core samples, 41 from cuttings, 2 from drilling mud, and 5 from side wall cores. Of the Inigok samples, 26 were from core samples, 44 from cuttings, 2 from drilling mud, and 10 from side wall cores. The N Inigok and W Kubaruk wells only contained cutting samples.

### **Seismic**

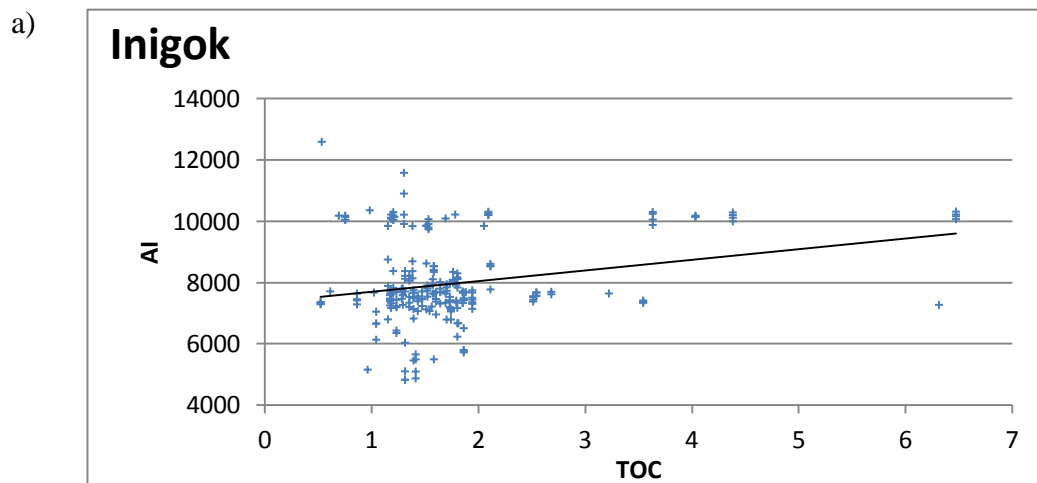
Seismic lines were imported from the National Archive of Marine Seismic Surveys – USGS PCMSC. Two series were selected for their proximity to the wells in the study. The first series, N-PR-81-AK, contained lines 22-81 and 27-81. The second series, W-40-80-AK

contained line 10X. Line 22-81 contained approximately 76 line kilometers of seismic data, line 27-81 contained approximately 65 line kilometers, and line 10X contained approximately 89 line kilometers. Series N-PR-81-AK (Appendix G) was shot by the USGS, Central Region, Energy Resources Team from 01/01/1981-01/17/1981. Series W-40-80-AK (Appendix H) was shot by Arco Group from 01/01/1980-02/10/1980.

## Analysis

### Plots

Four graphs presenting the plots of AI/TOC are found below, one for each of the wells. A fifth plot is presented combining the data for all of the wells. The acoustic impedance from the synthetic seismogram was given in units of ft/s  $\text{g}/\text{cm}^3$ . In order to be consistent with the Løseth et al [2011] plot, all AI values were converted to units of m/s  $\text{g}/\text{cm}^3$ . The TOC was given as a weight percent. Of the four wells, none showed the expected non-linear trend proposed by Løseth et al. [2011]. What was observed instead was a linear increase of AI with increasing TOC. Even when all the wells were combined into one graph the results had the same linear trend.





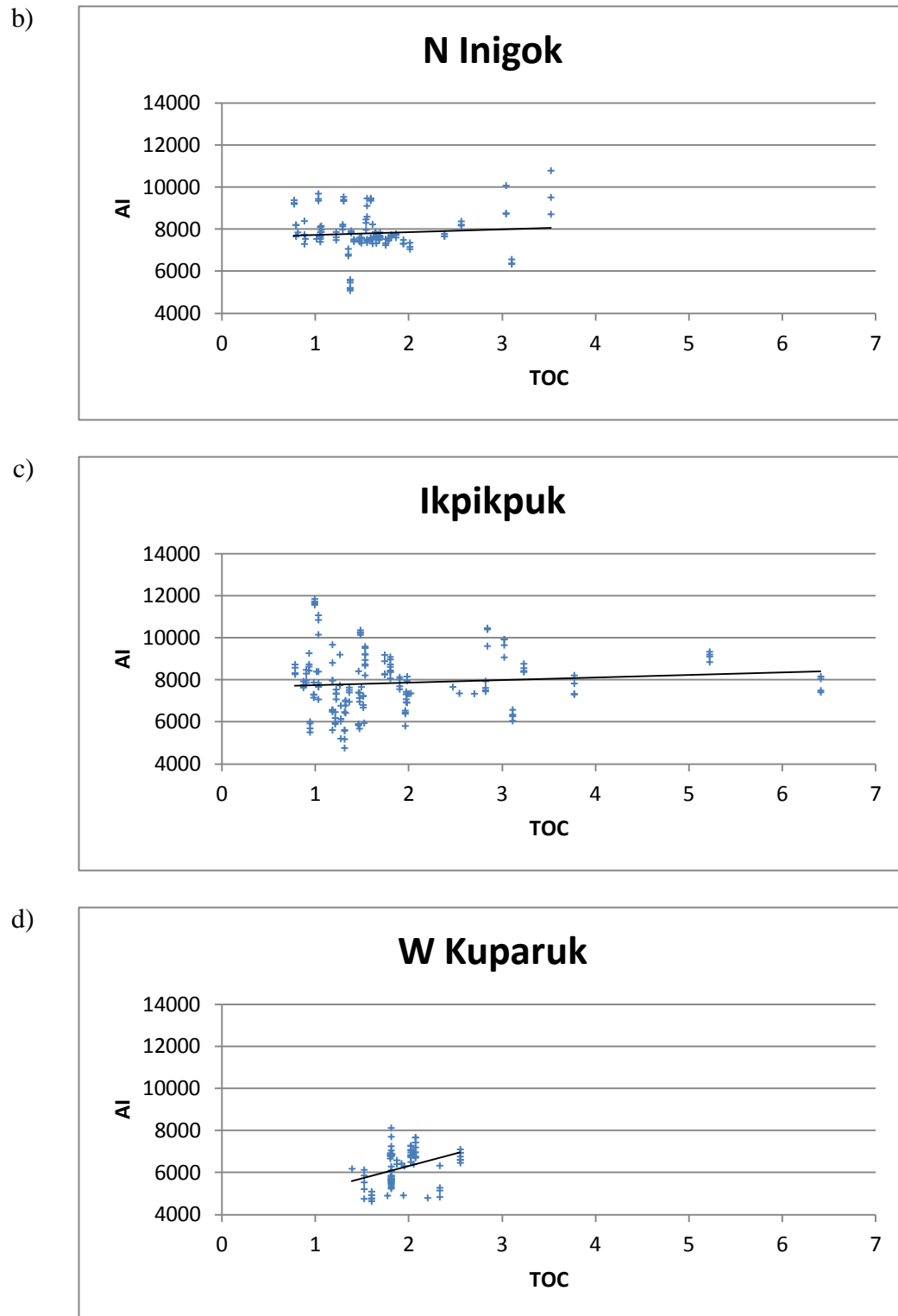


Figure 14: Individual plots for each of the well. All four wells indicated a trend of TOC increasing as AI increases.

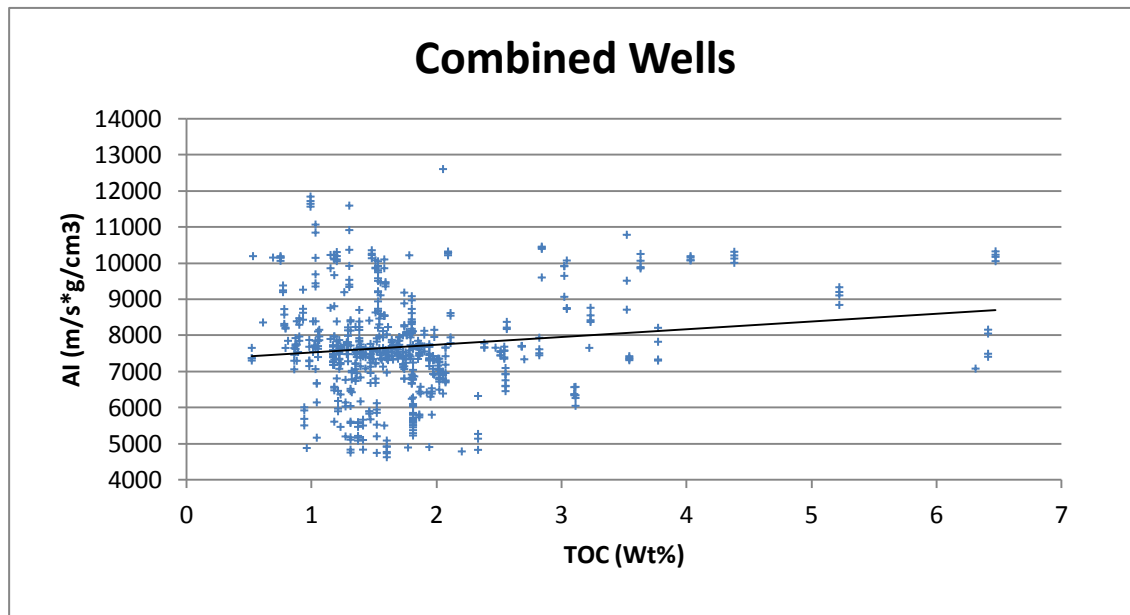


Figure 15: Plot showing data from all four wells combined.

### Seismic relationship

In the Løseth study a theoretical TOC curve was created using the resistivity and the sonic logs as proposed by Passey et al., [1990]. In my study the actual TOC was known at given depths from the USGS Database, therefore a simple plot of the TOC/depth was created for each of the wells. The most distinct plot showed that along the N Inigok well the highest concentration of TOC was at the base of the Kingak within the K1 minor sequence. The concept of applying the TOC curve to seismic could then be tested. According to Løseth et al. [2011] if the concentration of the TOC is at the base of the formation you should expect a strong positive reflection at the source rock base while the top negative reflection should be the weaker of the two. This was clearly observed along the seismic line and confirmed the expectation. However, as previously stated it has been determined that the N Inigok well is economically depleted [Peters et al., 2006]. What that means is that any hydrocarbons that are movable have moved

out of the source rock. Because the TOC values were actual and not theoretical this could be compared to the petrophysical analysis. This analysis confirmed that there are no remaining hydrocarbons in place. From this, it must be assumed that theoretical TOC values and their satisfactory correspondent seismic response are not sufficient alone to determine the viability of a shale unit as an unconventional prospect.

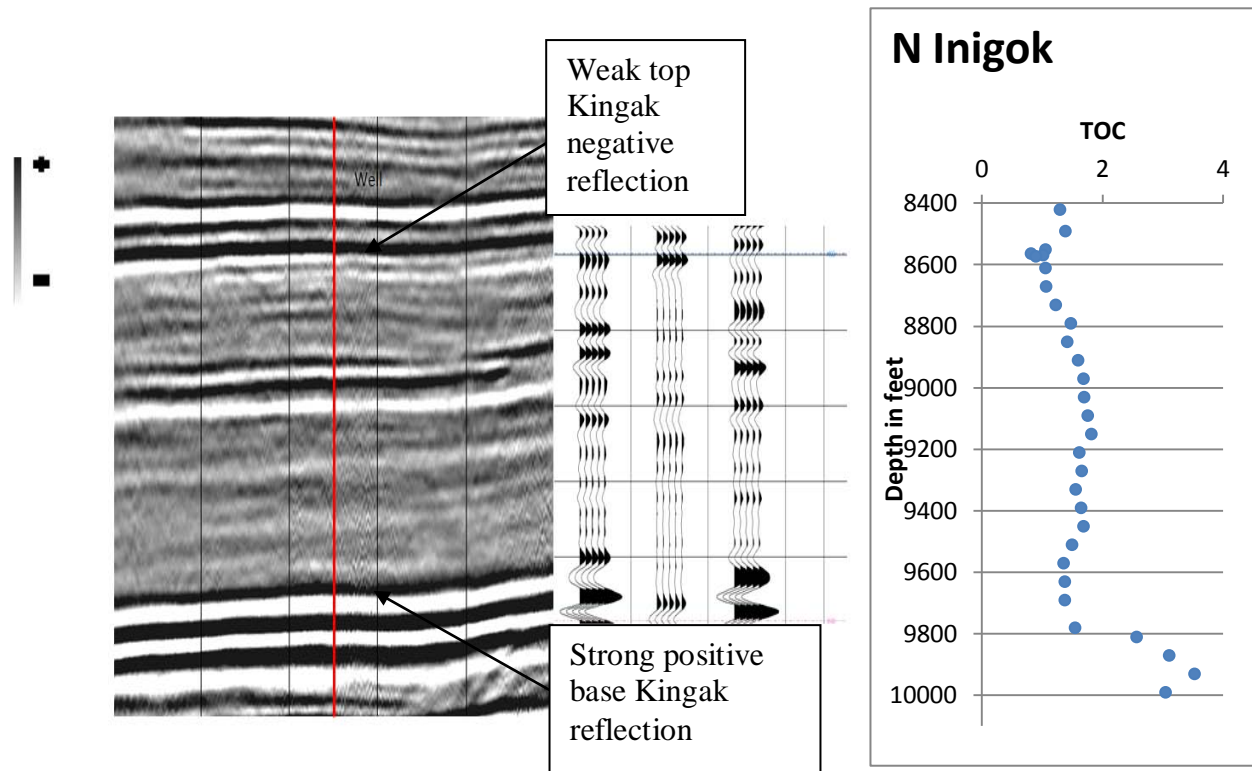


Figure 16: Seismic section along line 27-81 at the N Inigok well showing the weak top negative reflection and the strong positive base reflection. According to Løseth et al. [2011] this indicates a concentration TOC at the base of the shale. This was confirmed with a simple depth plot of TOC values.

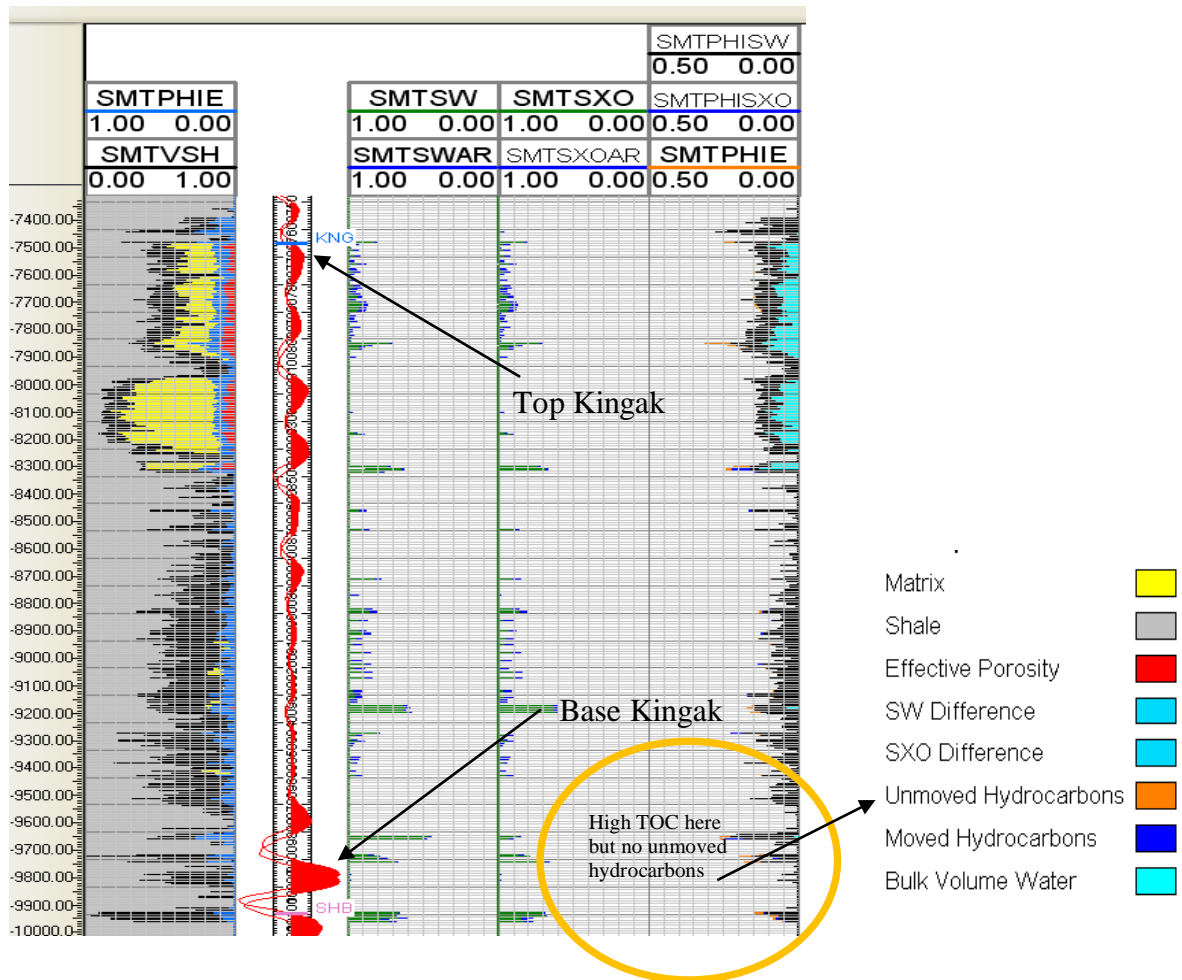


Figure 17: Petrophysical analysis of Kingak from N Inigok well logs showing absence of any remaining unmoved hydrocarbons. This indicates that the Løseth et al. [2011] method of identifying TOC concentration from seismic does not provide the necessary criteria to determine if the hydrocarbons are still extractable.

## Results

AI was plotted against TOC to observe the baseline trend for each of the wells. The trend was inconsistent with the predicted response as established by Løseth et al., [2011]. With regard to creating a baseline curve there are several possible reasons for the discrepancy observed. The first possibility is that the velocities are incorrect on the well logs. There were portions of the well logs that needed editing. This is because the original log did not begin until the instrument reached a certain depth down the hole. What was recorded was a false value of -

999 until the recording instrument was actually turned on. It was necessary to erase this portion of the log and set the values at zero. There were several points along each of the wells where these false values appeared indicating that the instrument had been turned off for a period of time. In each of these instances the values were again set to zero. This occurred in each of the wells and affected both the Sonic (DT) and Density (RHOB) log curves; both responsible for generating the AI curve. However, none of the final AI readings that were used were equal to zero; therefore this did not affect the AI curve for the Kingak shale. It is just unknown whether erasing (editing) portions of the log have an impact of the overall velocity.

Another potential problem with the comparison of my study to that of Løseth et al., [2011] is the integrity of the well to seismic correlation in my study. Visually the wells appeared to be a good fit to the seismic data. However, there were problems loading the seismic data into KINGDOM © the seismic lines and wells as a result are not geographically located. The seismic lines 22-81 and 27-81 had been used for the AAPG Imperial Barrel Award competition in 2012. The project was made available to the University of Texas at El Paso under a proprietary agreement with the AAPG. However, the seismic lines were geographically located in that instance, and as a result I could load the wells in that data set therefore obtaining a necessary visual approximation of where the wells sat along the seismic lines. In the case of the line 10X and the well W Kuparuk St 3-11-11, Google Earth was used to site where along the seismic line the well was located. From there the well log data and Formation Tops Inventory [Alaska Division of Geological & Geophysical Surveys (DGGs), 2012] were used to find the best-fit location. For this there is uncertainty particularly with regard to interpretations along line 10X. However, the synthetic seismogram is created from the well logs. The sonic log along the well is converted to depth. The Formation Tops were listed according to their depth

along the well. So this does not change the AI measurements reported. The uncertainty is only with regard to how well the log data was correlated to the seismic. Since the final step of inversion could not be completed for other reasons this factor is irrelevant with regard to the findings of this study.

The final and most likely cause for discrepancy is that the majority of the TOC samples in my data set were taken from cuttings. In the case of a cuttings sample, the ground rock is brought to the surface and collected in a bin. It is from this bin that a single sample is collected and brought to the lab for Rock-Eval Pyrolysis. The larger the sample interval is, the less likely the results from one collection will apply to the length of the interval. It was found that in one instance the interval was 73m. The actual thickness of the Kingak along this well was 552m, therefore the 73m sample represented roughly 13% of the entire formation and assigned only one TOC value. In the case of wells with smaller (9m) intervals it was observed that a TOC values could increase/decrease by as much as 5-6% from one interval to another. Furthermore, the synthetic seismogram recorded changes in AI at roughly 3m intervals. Because any intervals of the formation greater than 3m were assigned multiple AI values for only one TOC value it is highly probable that this led to the inconsistent results that were observed. For the sake of comparison I also plotted the average AI along the interval so that a single TOC value was matched to a single AI value. This did not change the results. It is clear that average values or values obtained from intervals greater than the AI measurements from the synthetic seismogram have the potential to alter the baseline curve.

The trend that was observed in this study was consistent in each of the wells; specifically a linear trend of increasing TOC with increasing AI. Several different trend lines were applied to the plots, however none seemed to bear any resemblance to the *Løseth* curves (see Appendix

I). It was only when I removed all data points except those from single depth sources such as cores that I began to see the emergence of a curve using a logarithmic trend line (Appendix J). This, to some degree, confirms my conclusion that single depth sources are necessary for accurate curve calculation. At this time it does not appear that the level of maturity had any effect the trend of the plot. In the case of the visual match of the TOC curve to the seismic response, maturity again did not appear to affect the outcome. However, it was observed, that reflection strength did not indicate in place hydrocarbons.

### **Future Work**

This study did not yield the expected results and it is possible that more control on the TOC sampling method would yield better results. Future work should be undertaken using samples only from core analysis, not cuttings. The interval for each sample should be lengths consistent with the changes recorded for the AI on the synthetic seismogram (i.e. 10 feet). For the most consistent results core samples should be used. In addition, with improved seismic processing (removal of noise, and geographically locating the data set) a greater degree of confidence will be obtained. Future work should continue to explore the relationship between the seismic amplitude response and high TOC locations within the shale specifically considering level of maturity if this technique can ever be successfully applied remotely without the necessity of drilling several wells.

### **Summary**

The ability to obtain information about the quality of source rock is of increasing importance as petroleum exploration moves into more remote locations than ever before. The study presented by Løseth et al., [2011] has all the necessary elements for this type of evaluation. At this point it does not appear to allow the interpreter to evaluate the shale remotely from just

seismic data as was hoped. Rather, a combination of well logs, seismic data, and rock-eval pyrolysis is still necessary. A continuation of the development of this process will greatly contribute to future oil reserves and perhaps eliminate the necessity of one or more of the costly processes in determining the viability of the unconventional prospect.

## Works Cited

Alaska Division of Geological & Geophysical Surveys (DGGS). *Formation Tops Inventory by Well*. (2012): [http://www.dggs.alaska.gov/gmc\\_inventory/google\\_earth/inventory/Alaska-GMC-Formation-Tops.pdf](http://www.dggs.alaska.gov/gmc_inventory/google_earth/inventory/Alaska-GMC-Formation-Tops.pdf).

Ashcroft, W. (2011), *A Petroleum Geologist's Guide to Seismic Reflection*. Wiley-Blackwell, West Sussex, UK.

Bailey, A., *Conoco Keeps the Oil Flowing*. (2010).  
<http://www.pertroleumnews.com/pnads/601168964.shtml>.

Handschy, J. W. (1998). Regional Stratigraphy of the Brooks Range and North Slope, Arctic Alaska: Special Paper 324. In: J. S. Oldow & H. G. Ave Lallemand, eds. *Architecture of the Central Brooks Range Fold and Thrust Belt*. Boulder: The Geological Society of America, pp. 1-8.

Houseknecht, D. & Bird, K. (2004). Sequence Stratigraphy of the Kingak Shale (Jurassic-Lower Cretaceous), National Petroleum Reserve in Alaska. *AAPG Bulletin*, March, 88(3), pp. 279-302.

Houseknecht, D., Rouse, W., Garrity, C., Whidden, K., Dumoulin, J., Schenk, C., Charpentier, R., Cook, T., Gaswirth, S., Kirschbaum, M., Pollastro, R., (2012). *Assessment of Potential Oil and Gas Resources in Source Rocks of the Alaska North Slope, 2012*, Fairbanks: USGS.

Houseknecht, D. W. (2001). *Sequence Stratigraphy and Sedimentology of Beaufortian Strata (Jurassic - Lower Cretaceous) in the national Petroleum Reserve - Alaska (NPRA. s.l., SEPM Core Workshop*, pp. 57-88.

Houseknecht, D. W. (2012). *Personal communication*.

Løseth, H., Wensaas, L., Gading, M., Duffaut, K., Springer, M., (2011). Can Hydrocarbon Source Rocks be Identified on Seismic Data. *Geology*, December, 39(12), pp. 1167-1170.

Mull, C. G., Roeder, D. H., TAILLEUR, I. L., Pessel, G. H., Grantz, A., May, S. D., (1987). *Regional Geology of the North Slope of Alaska*. [http://dog.dnr.alaska.gov/GIS/Data/NSResourceSeries/NorthSlope\\_Resource\\_Series\\_Regional\\_Geology.pdf](http://dog.dnr.alaska.gov/GIS/Data/NSResourceSeries/NorthSlope_Resource_Series_Regional_Geology.pdf).



Passey, Q. R., Creaney, S., Kulla, J. B., Moretti, F. J., Stroud, J. D., (1990). A Practical Model for Organic Richness from Porosity and Resistivity Logs. *AAPG Bulliten*, December, 74(12), pp. 1777-1794.

Peters, K., Magoon, L., Bird, K., Valin, Z., Keller, M., (2006). North Slope, Alaska: Source Rock Distribution, Richness, Thermal Maturity, and Petroleum Charge. *AAPG Bulliten*, February, 90(2), pp. 261-292.

State of Alaska Department of Natural Resources: Alaska Geologic Materials Center (2009). *Data Report No. 361 X-ray Diffraction Analysis of Various Wells*, s.l.: State of Alaska.

State of Alsaka (2011). *Division of Oil and Gas*.  
<http://dog.dnr.alaska.gov/ResourcesEvaluation/ResourceEvaluation.html>.

TAMU, 2011. *Rock Eval Pyrolysis*. [http://www-opd.tamu.edu/publications/tnotes/tn30/tn30\\_11.htm](http://www-opd.tamu.edu/publications/tnotes/tn30/tn30_11.htm)

Thomas, C. P., Faulder, D. D., Doughty, T. C., Hite, D. M., White, G. J., (2007). *Alaska North Slope Oil and Gas a Promising Future or an Area in Decline? DOE/NETL - 2007/1280*, Fairbanks: National Energy and Technology Laboratory / Department of Energy.

US Department of the Interior (2011). *pubs*.<http://pubs.usgs.gov/of/1999/ofr-99-0015/Wells>.

USGS (1974-1981). *National Archive of Marine Seismic Surveys*. <http://walrus.wr.usgs.gov/NAMSS/>

## Appendix

### Appendix A: Table of Sample Type

Ikpikpuk		Inigok		N Inigok		3/11/2011	
Samp ID	Style	Samp ID	Style	Samp ID	Style	Samp ID	Style
9502792000400000259	CC	9502792000300000367	CC	9502792000300000406	CT	9501032001700000253	CT
9502792000400000260	CC	9502792000300000402	CC	9502792000300000408	CT	9501032001700000255	CT
9502792000400000261	CC	9502792000300000436	CC	9502792000300000412	CT	9501032001700000257	CT
9502792000400000262	CT	9502792000300000476	CC	9502792000300000414	CT	9501032001700000259	CT
9502792000400000264	CT	9502792000300000478	CC	9502792000300000416	CT	9501032001700000261	CT
9502792000400000266	CT	9502792000300000480	CC	9502792000300000420	CT	9501032001700000263	CT
9502792000400000268	CT	9502792000300000482	CC	9502792000300000422	CT	9501032001700000265	CT
9502792000400000270	CT	9502792000300000483	CC	9502792000300000424	CT	9501032001700000267	CT
9502792000400000272	CT	9502792000300000485	CC	9502792000300000428	CT	9501032001700000269	CT
9502792000400000274	CT	9502792000300000486	CC	9502792000300000430	CT	9501032001700000271	CT
9502792000400000276	CT	9502792000300000487	CC	9502792000300000432	CT	9501032001700000273	CT
9502792000400000278	CT	9502792000300000488	CC	9502792000300000437	CT	9501032001700000275	CT
9502792000400000280	CT	9502792000300000489	CC	9502792000300000441	CT	9501032001700000277	CT
9502792000400000283	CT	9502792000300000491	CC	9502792000300000443	CT	9501032001700000279	CT
9502792000400000285	CT	9502792000300000492	CC	9502792000300000447	CT	9501032001700000282	CT
9502792000400000287	CT	9502792000300000494	CC	9502792000300000449	CT	9501032001700000284	CT
9502792000400000289	CT	9502792000300000495	CC	9502792000300000453	CT	9501032001700000285	CT
9502792000400000291	CT	9502792000300000496	CC	9502792000300000455	CT	9501032001700000286	CT
9502792000400000293	CT	9502792000300000497	CC	9502792000300000457	CT	9501032001700000287	CT
9502792000400000295	CT	9502792000300000498	CC	9502792000300000387	MD	9501032001700000289	CT
9502792000400000298	CT	9502792000300000500	CC	9502792000300000445	MD	9501032001700000291	CT
9502792000400000300	CT	9502792000300000501	CC	9502792000300000463	SW	9501032001700000293	CT
9502792000400000303	CT	9502792000300000503	CC	9502792000300000464	SW	9501032001700000295	CT
9502792000400000305	CT	9502792000300000504	CC	9502792000300000465	SW	9501032001700000297	CT
9502792000400000308	CT	9502792000300000506	CC	9502792000300000468	SW	9501032001700000299	CT
9502792000400000310	CT	9502792000300000342	CT	9502792000300000469	SW	9501032001700000301	CT
9502792000400000312	CT	9502792000300000344	CT	9502792000300000470	SW	9501032001700000303	CT
9502792000400000314	CT	9502792000300000346	CT	9502792000300000471	SW	9501032001700000305	CT
9502792000400000317	CT	9502792000300000348	CT	9502792000300000472	SW	9501032001700000307	CT
9502792000400000320	CT	9502792000300000350	CT	9502792000300000473	SW	9501032001700000309	CT
9502792000400000322	CT	9502792000300000352	CT	9502792000300000474	SW	9501032001700000311	CT
9502792000400000325	CT	9502792000300000354	CT			9501032001700000313	CT
9502792000400000327	CT	9502792000300000356	CT			9501032001700000315	CT
9502792000400000330	CT	9502792000300000358	CT			9501032001700000317	CT
9502792000400000333	CT	9502792000300000360	CT			9501032001700000319	CT
9502792000400000335	CT	9502792000300000362	CT			9501032001700000321	CT
9502792000400000338	CT	9502792000300000364	CT			9501032001700000323	CT
9502792000400000342	CT	9502792000300000366	CT			9501032001700000325	CT
9502792000400000344	CT	9502792000300000369	CT			9501032001700000328	CT
9502792000400000346	CT	9502792000300000371	CT			9501032001700000329	CT
9502792000400000349	CT	9502792000300000375	CT			9501032001700000331	CT
9502792000400000352	CT	9502792000300000377	CT			9501032001700000333	CT
9502792000400000355	CT	9502792000300000379	CT			9501032001700000335	CT
9502792000400000306	MD	9502792000300000383	CT				
9502792000400000315	MD	9502792000300000385	CT				
9502792000400000373	SW	9502792000300000389	CT				
9502792000400000374	SW	9502792000300000391	CT				
9502792000400000375	SW	9502792000300000395	CT				
9502792000400000376	SW	9502792000300000397	CT				
9502792000400000377	SW	9502792000300000401	CT				

*Samp ID:* unique ID given to each sample

*Style:* style sample drawn from

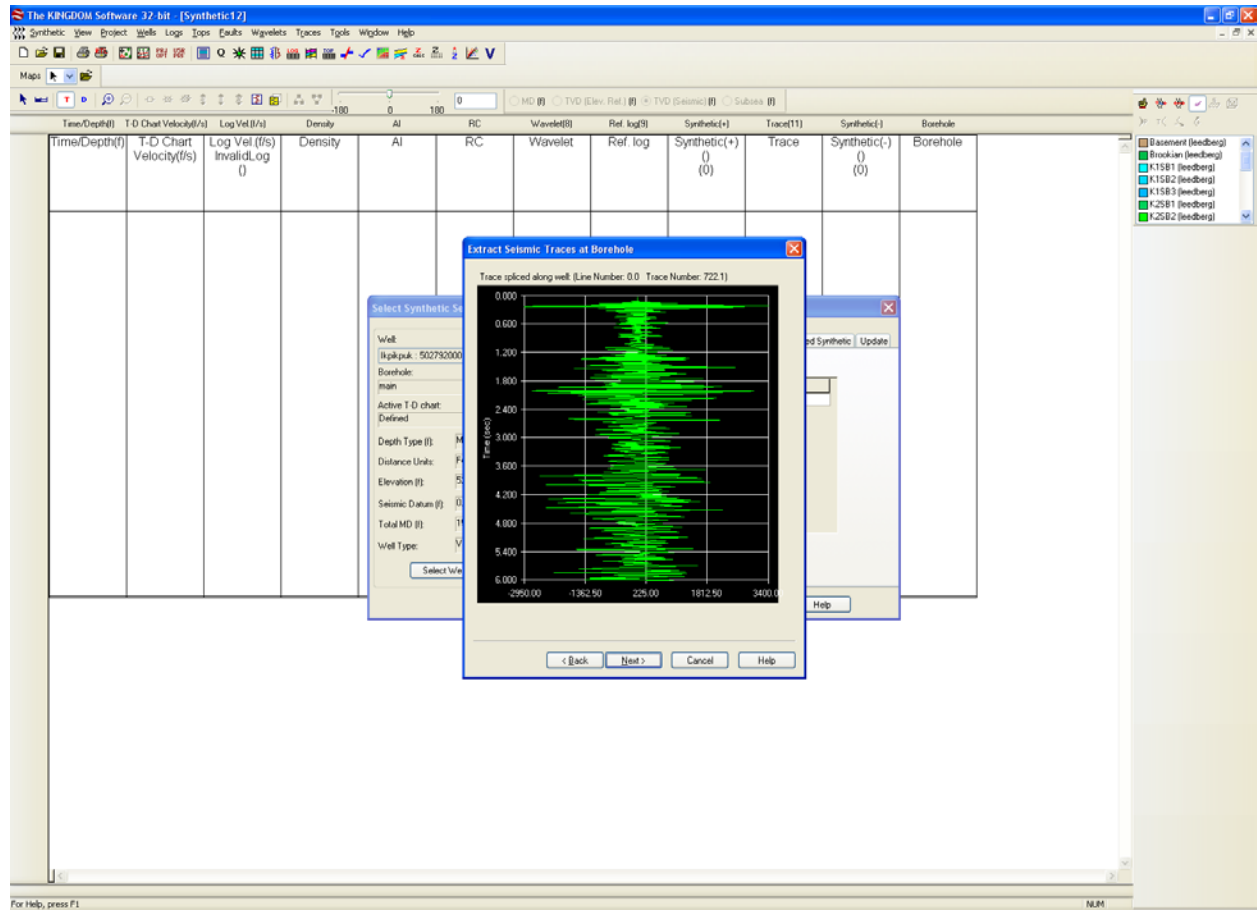
CC: Core Sample

CT: Cutting Sample

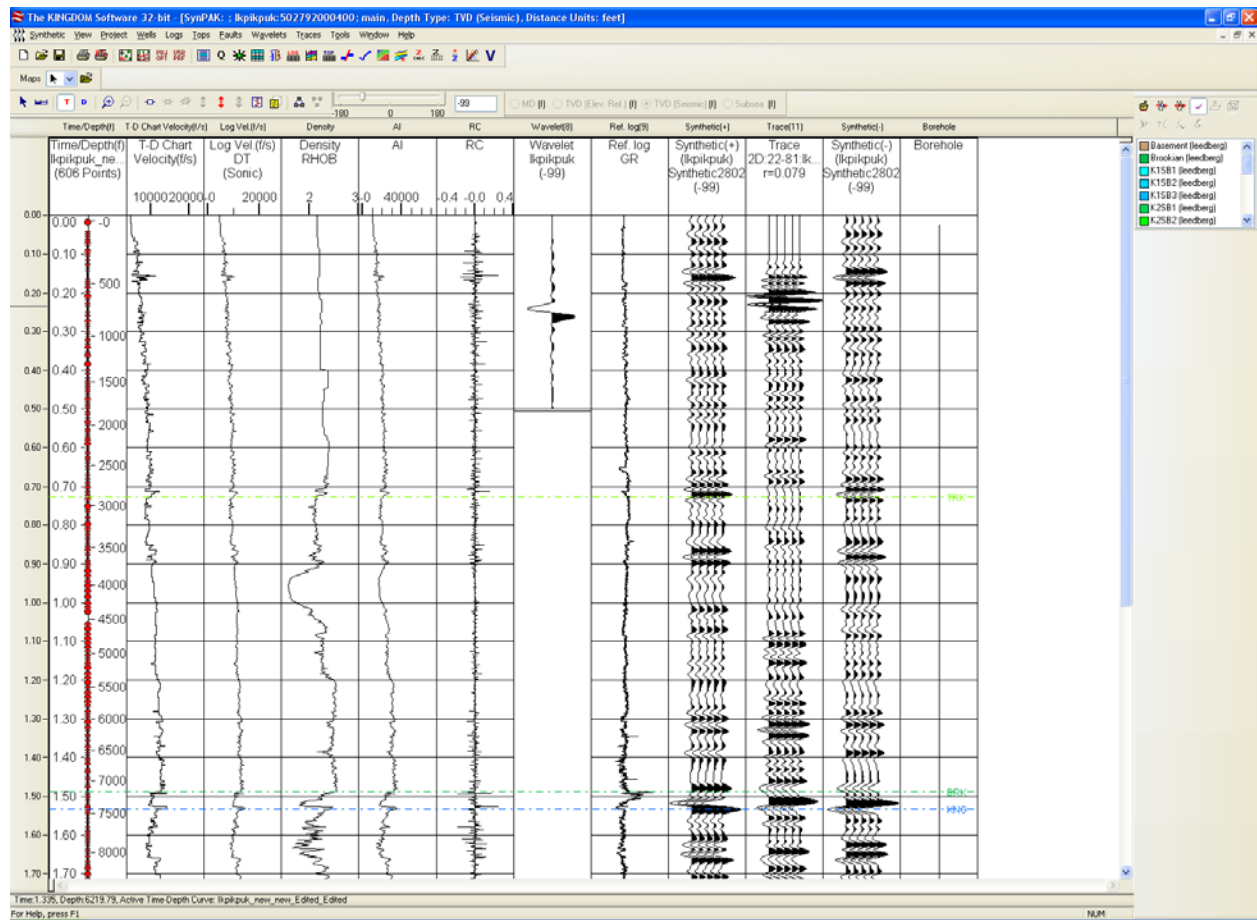
MD: Drilling Mud Sample

SW: Side Wall Core Sample

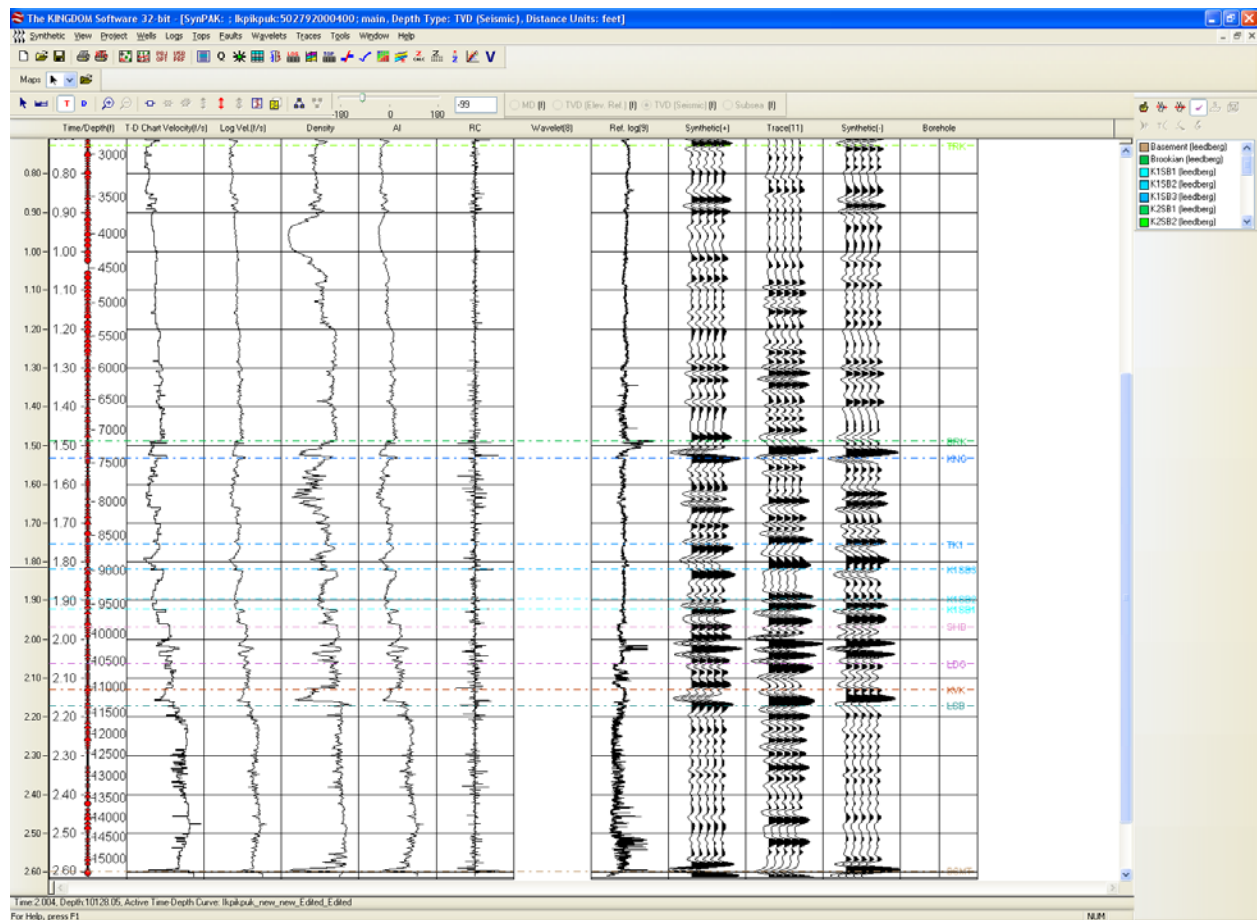
## Appendix B: Ikpikpuk



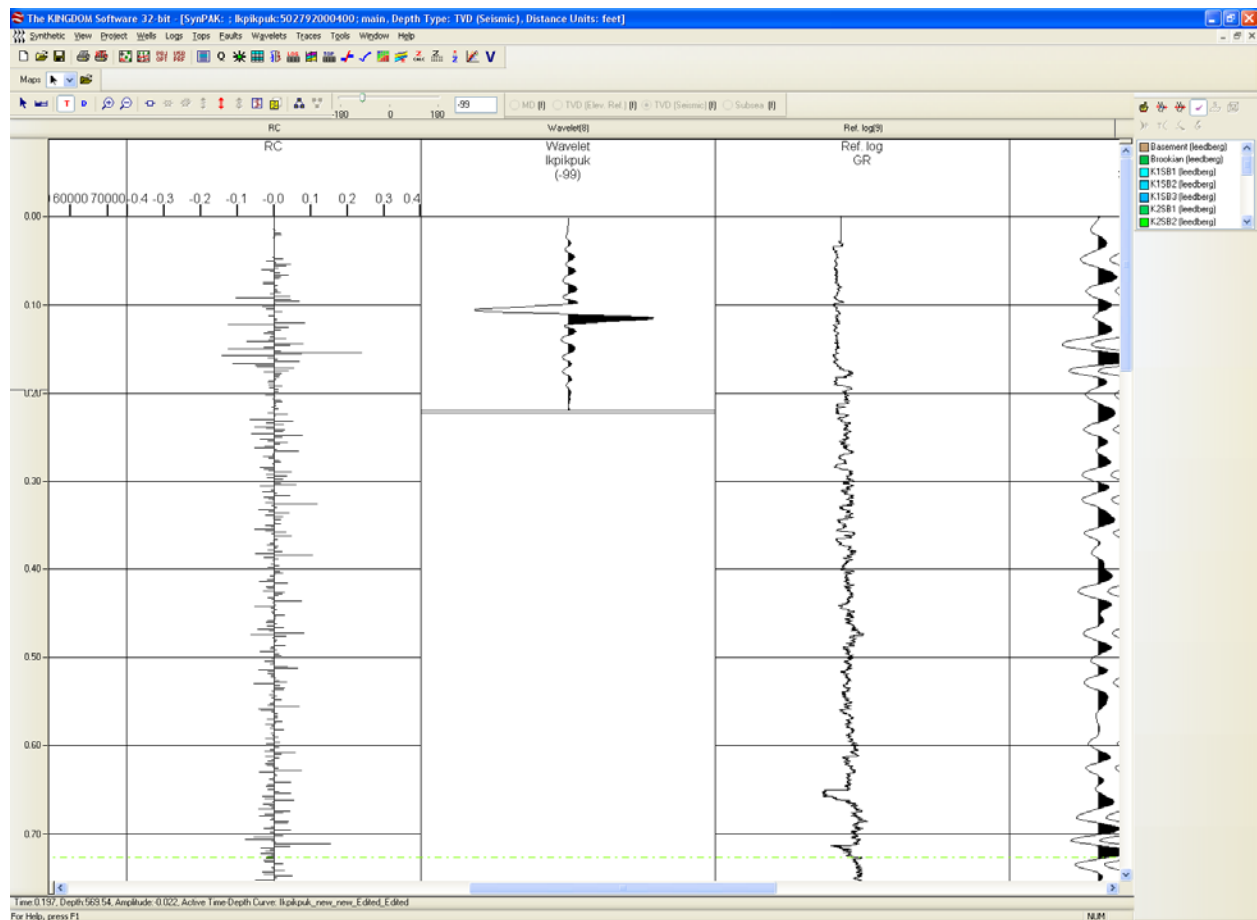
Screen Shot from KINGDOM © showing the extracted trace from along the borehole of the Ikpikpuk well.



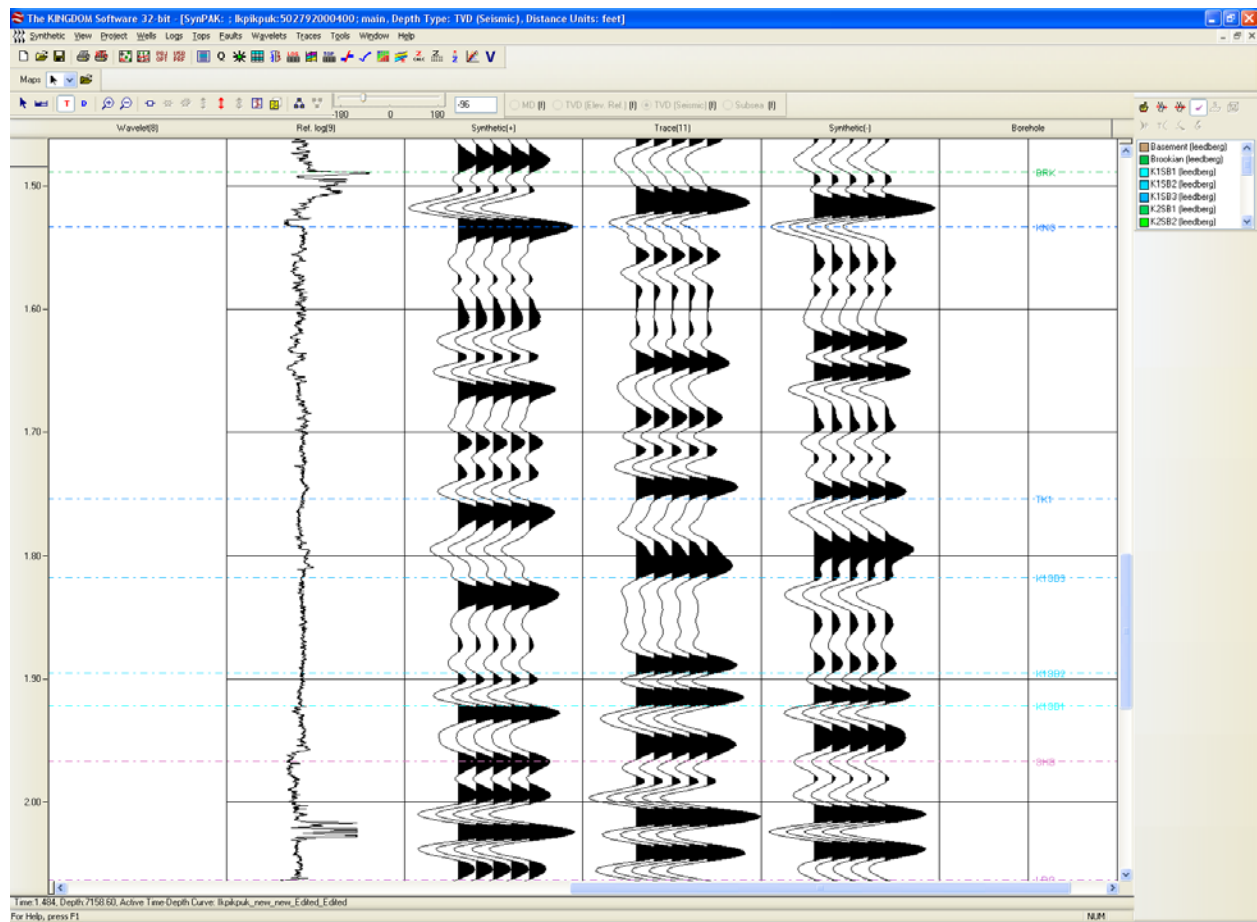
Screen shot from KINGDOM© top of the Ikpikpuk Synthetic Seismogram Wavelet rotated - 99 for best fit



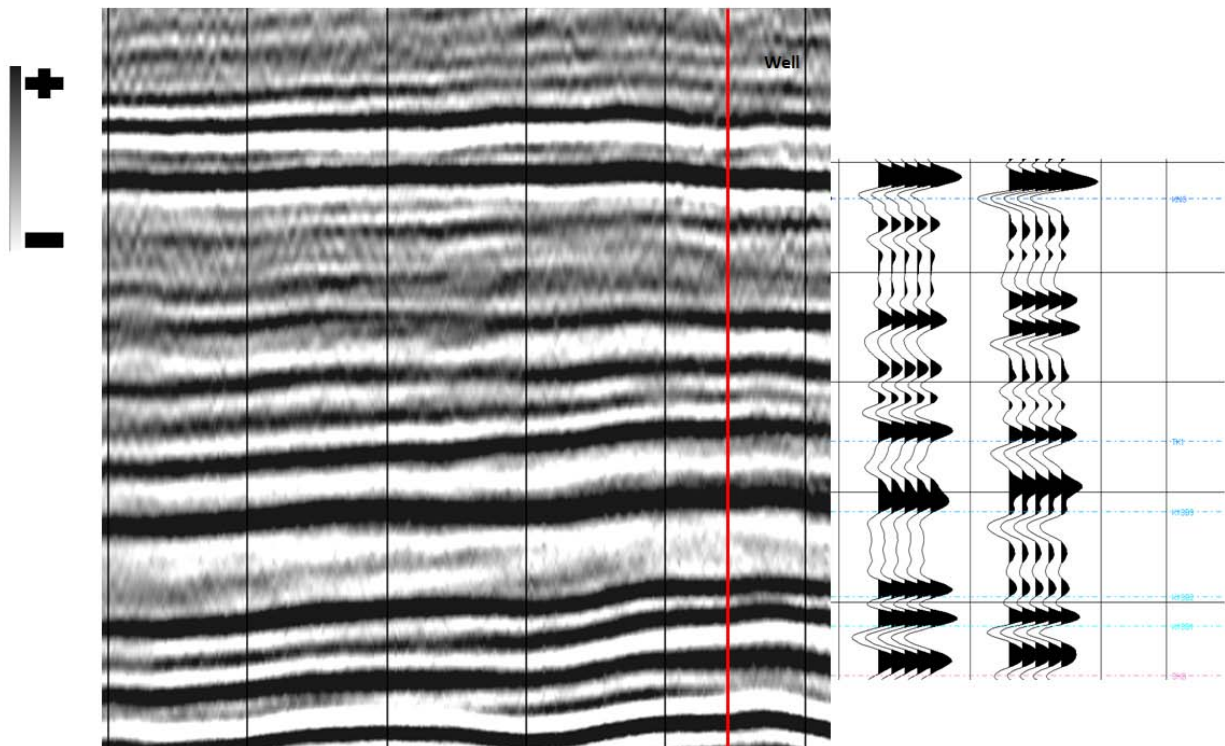
Screen shot from KINGDOM© bottom of Ikpikpuk Synthetic Seismogram showing Kingak formation. Wavelet Rotated -99 for best fit



Screen shot from KINGDOM© enlargement of Ikpikpak Wavelet rotated -99. Some noise was transferred during extraction due to seismic quality.

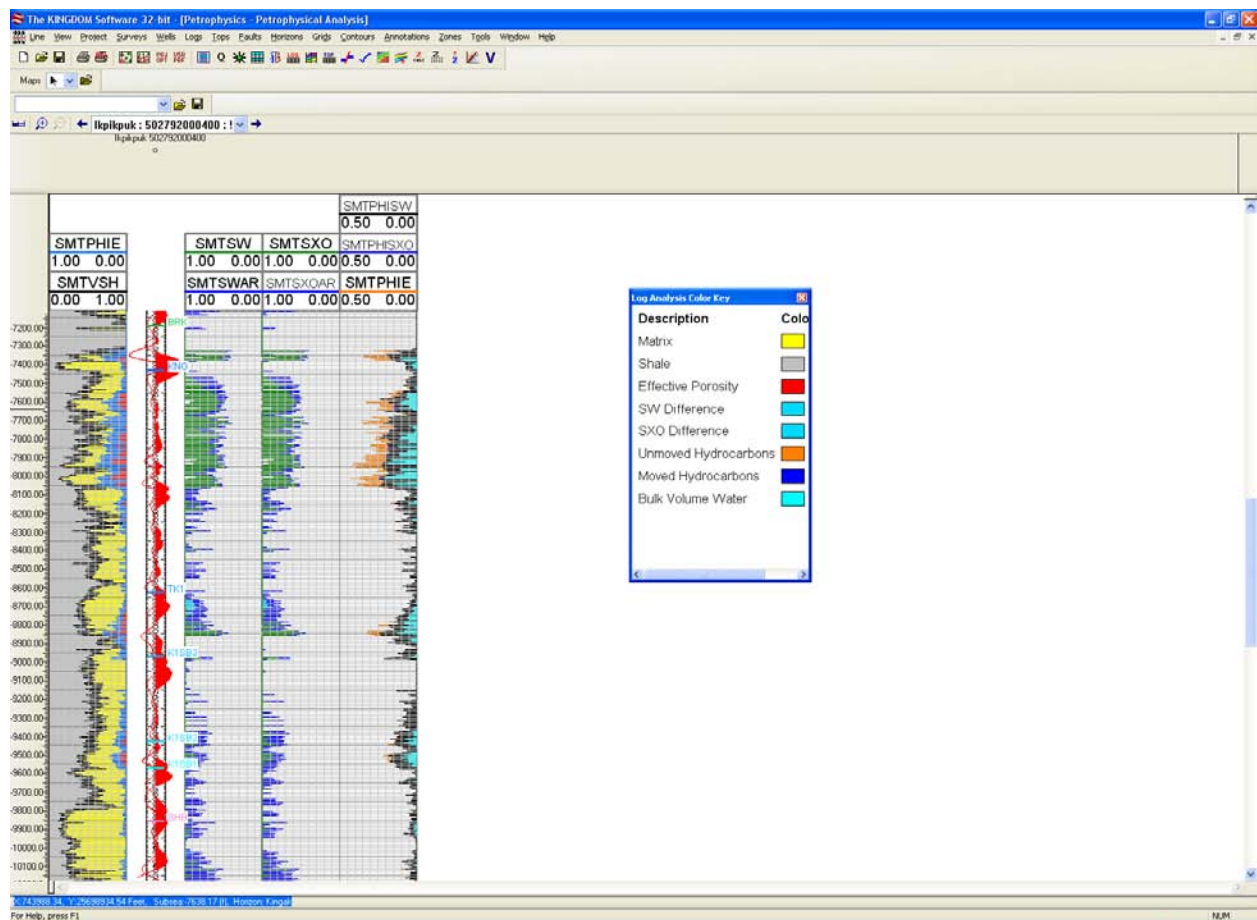


Screen shot from KINGDOM© enlargement of close correlation between extracted trace and the one generated by the Synthetic Seismogram



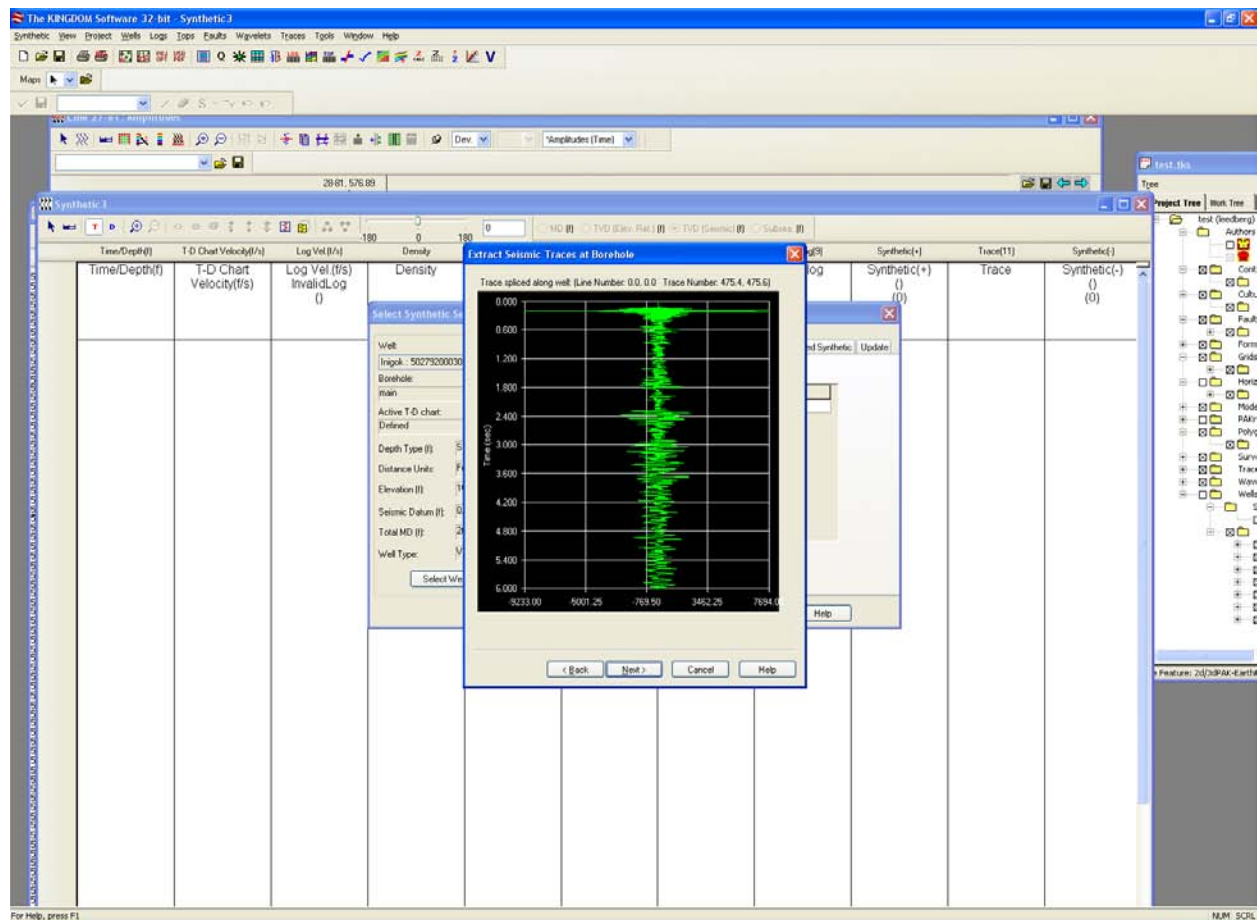
Extracted Trace and Synthetic Trace shown next to seismic section.  
Red line indicates position of the Ikpikpuk well.



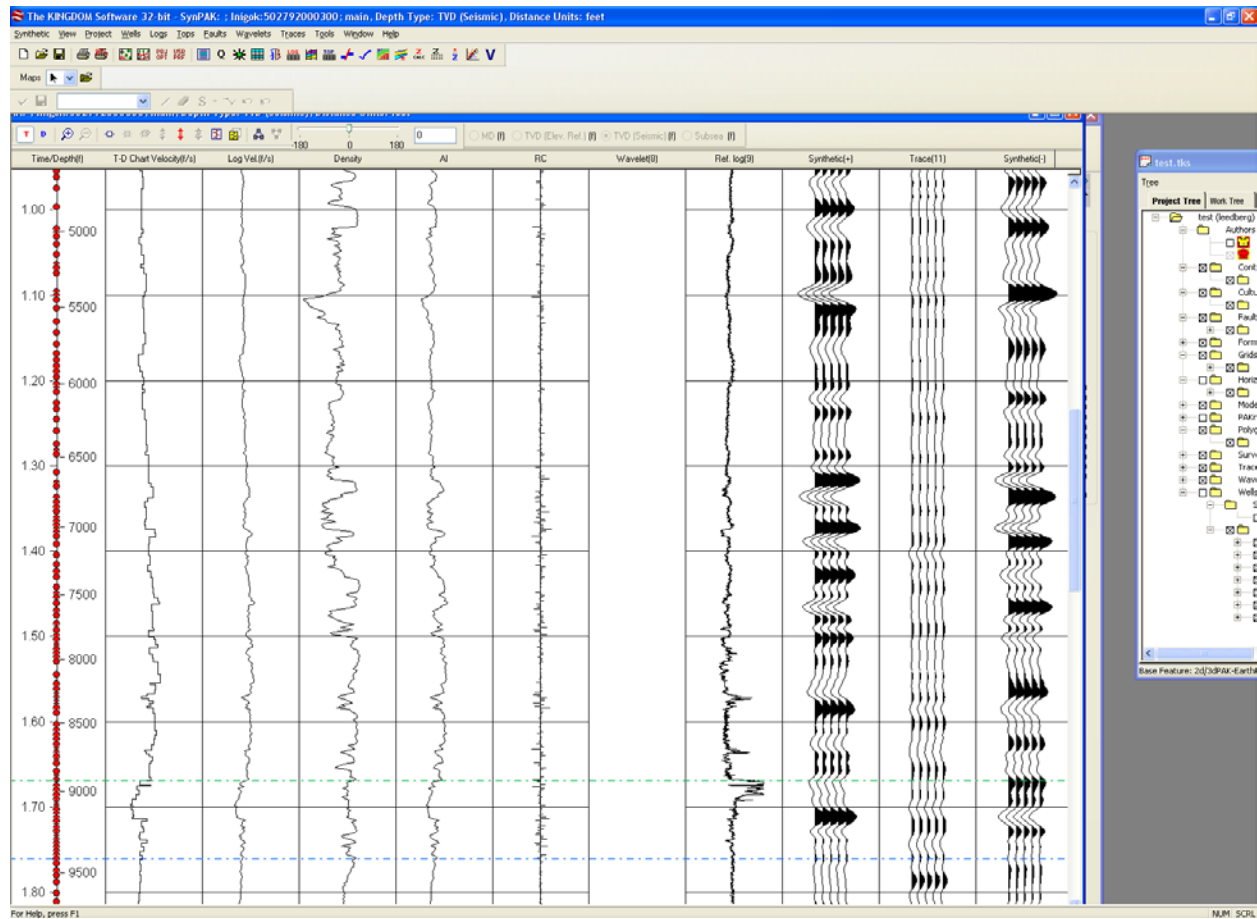


Screen shot from KINGDOM© of petrophysical analysis within the Kingak along the Ikpikpuk well.

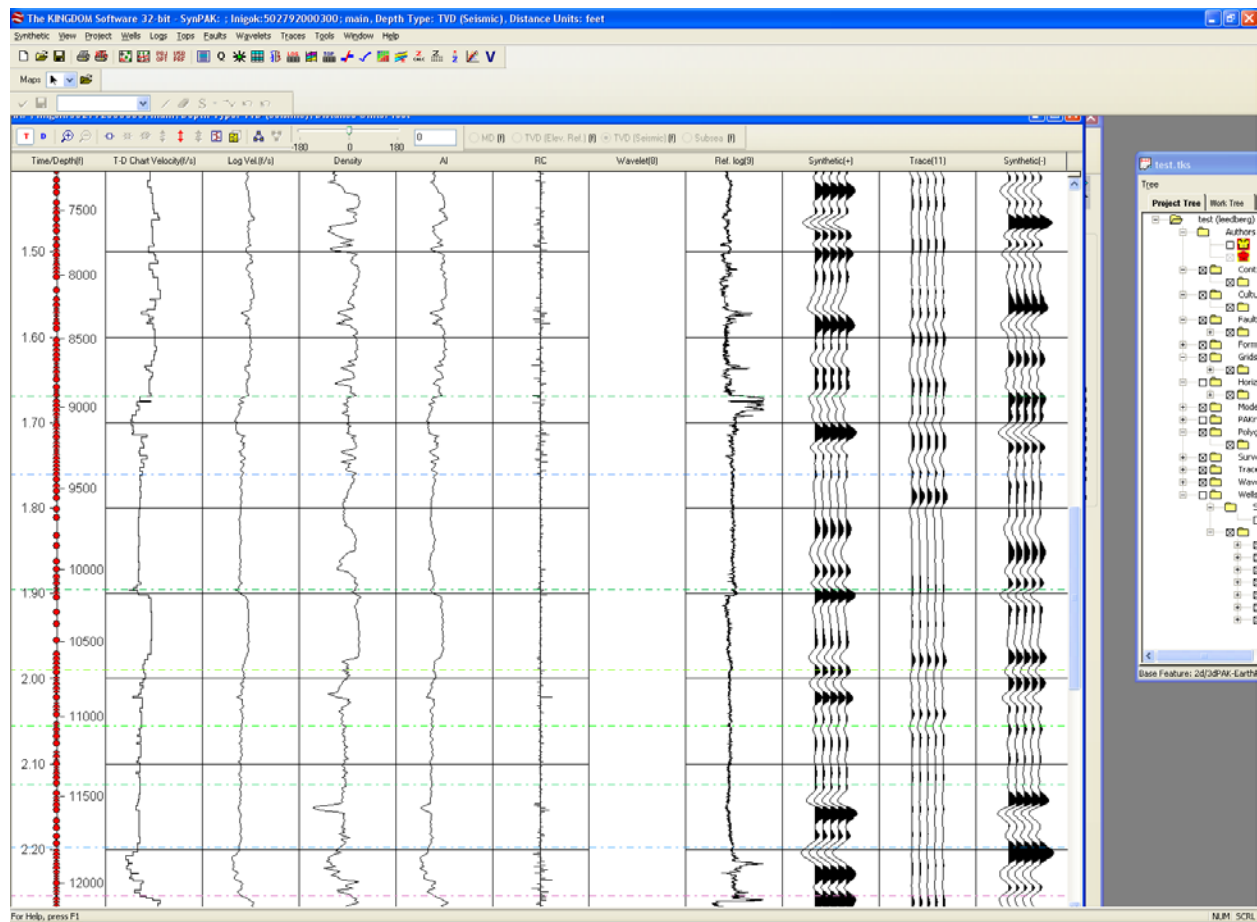
## Appendix C: Inigok



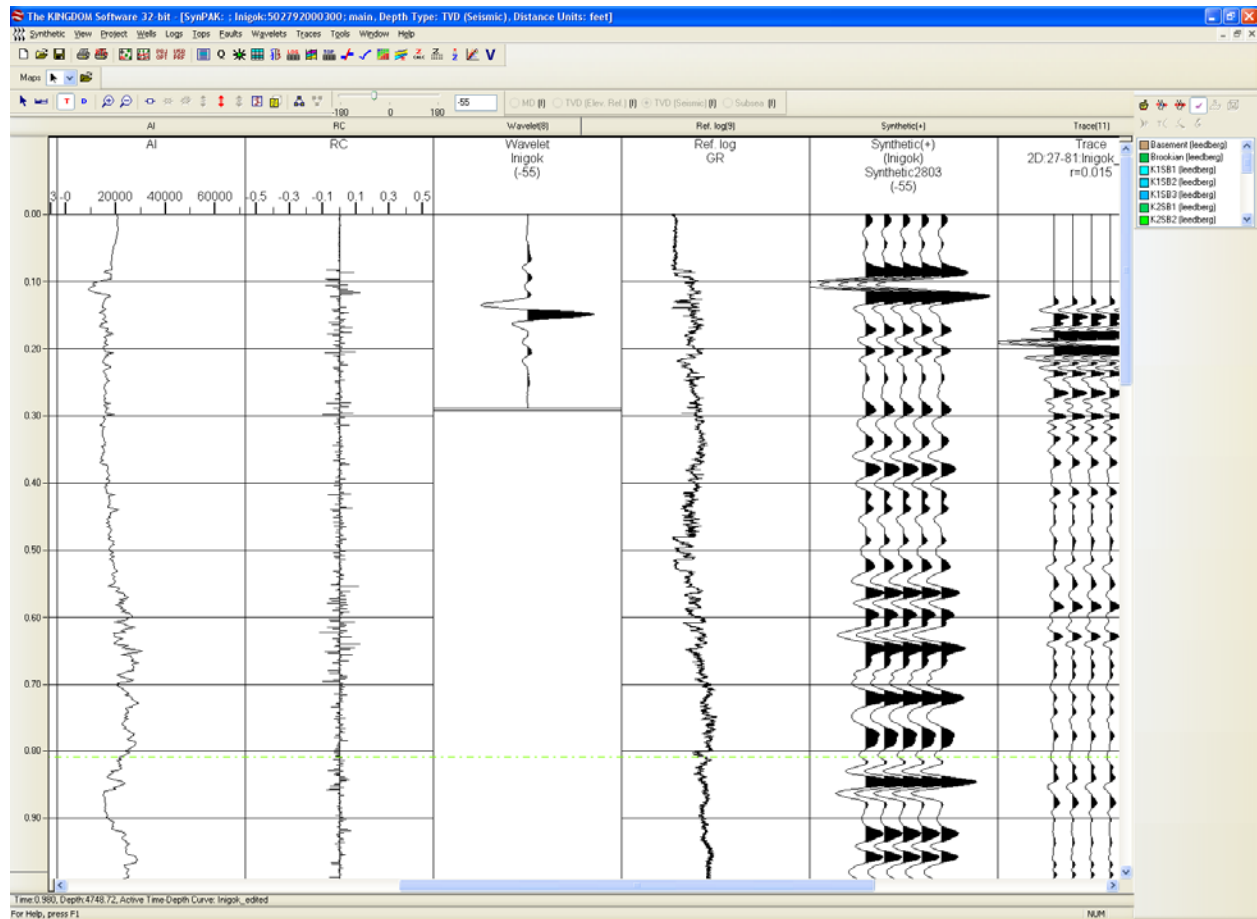
Screen Shot from KINGDOM© showing the extracted trace from along the borehole of the Inigok well.



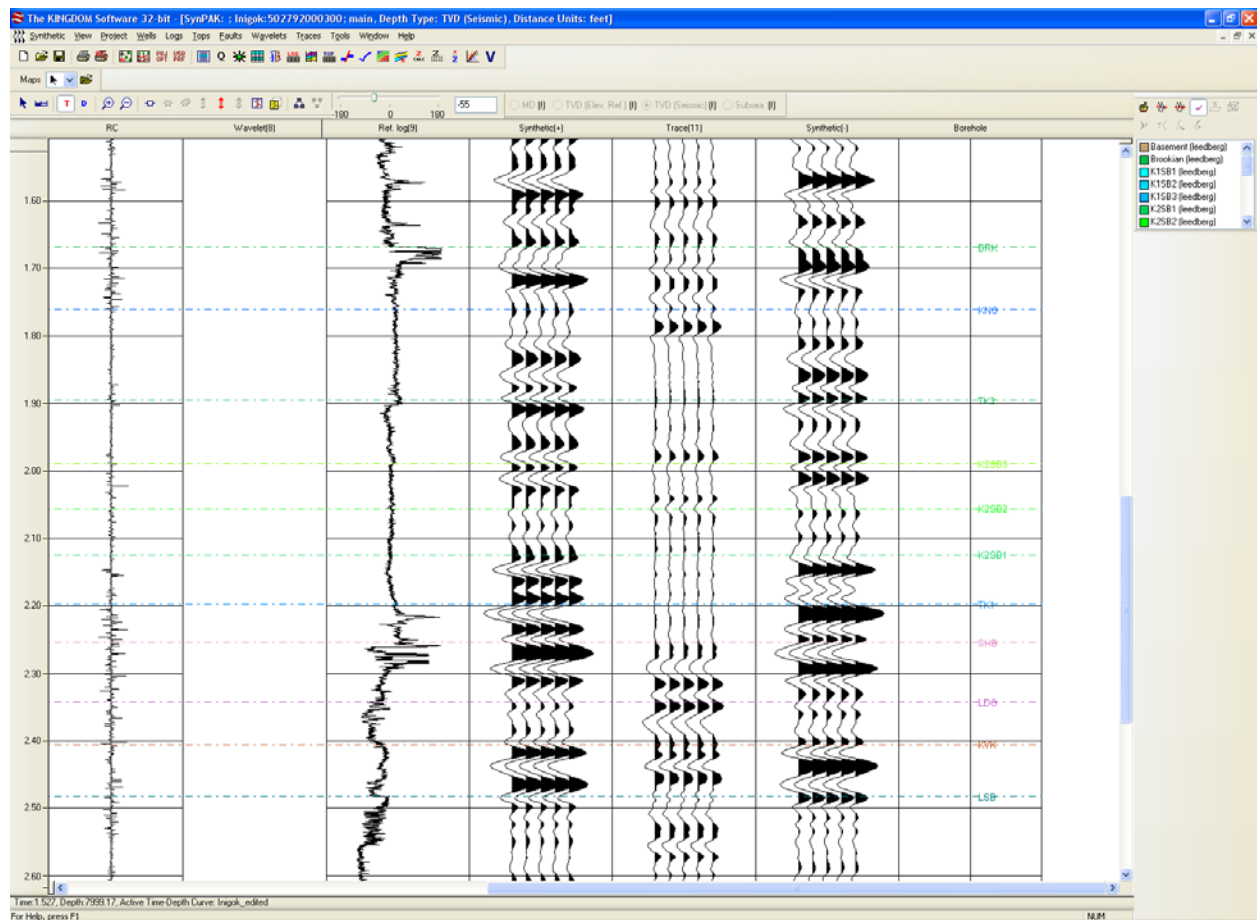
Screen Shot from KINGDOM© top of the Synthetic Seismogram generated from the Inigok well data.



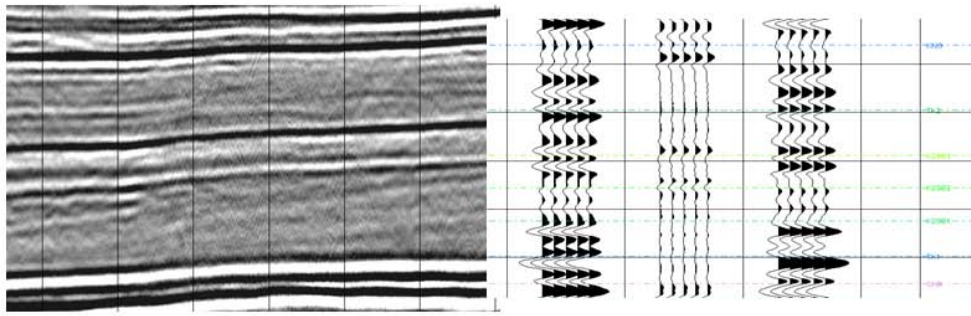
Screen Shot from KINGDOM© bottom of the Synthetic Seismogram generated from the well data of the Inigok well.



Screen Shot from KINGDOM© enlargement of the Wavelet extracted from the seismic section along the well. Wavelet was rotated -55 for a best fit. Some noise was transferred during extraction due to poor seismic quality.

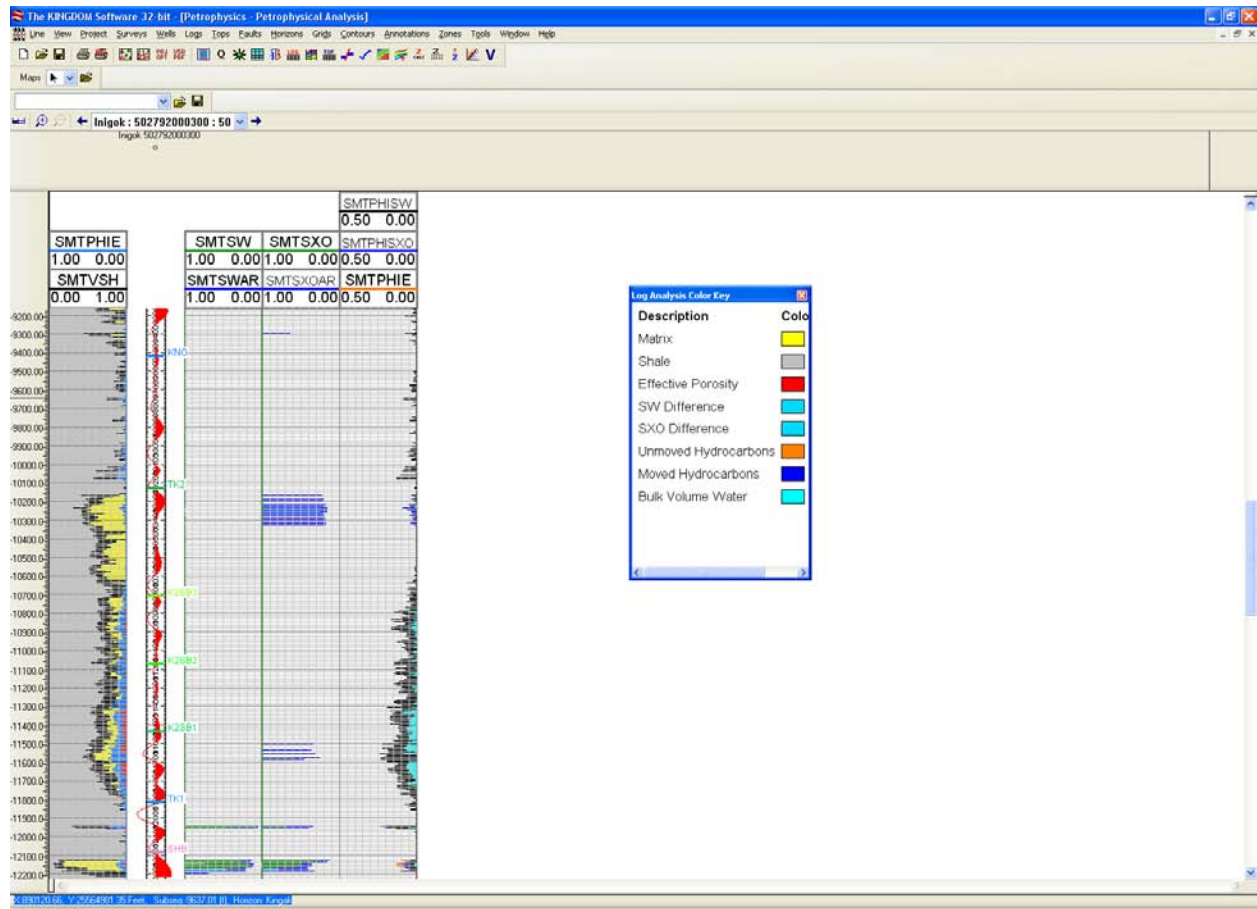


Screen Shot from KINGDOM© in spite of low amplitude reflections the correlation between the extracted trace and the Synthetic (+) trace is a good match. Green lines represent the minor sequence boundaries within the K2 sequence set identified using the gamma ray log as proposed by Houseknecht and Bird, 2004.



Seismic section showing the correlation between the seismic display and the Synthetic Seismogram along the Inigok well.

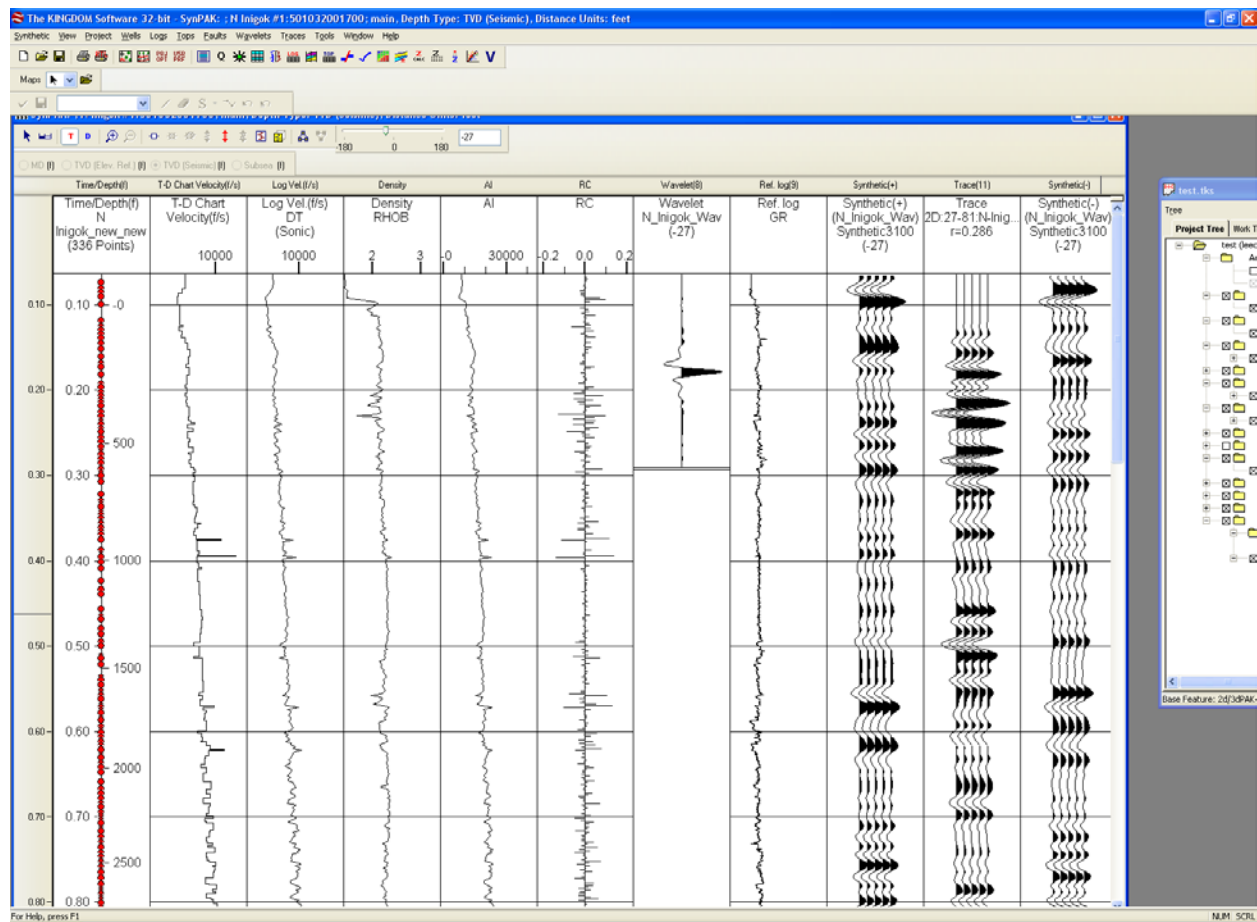




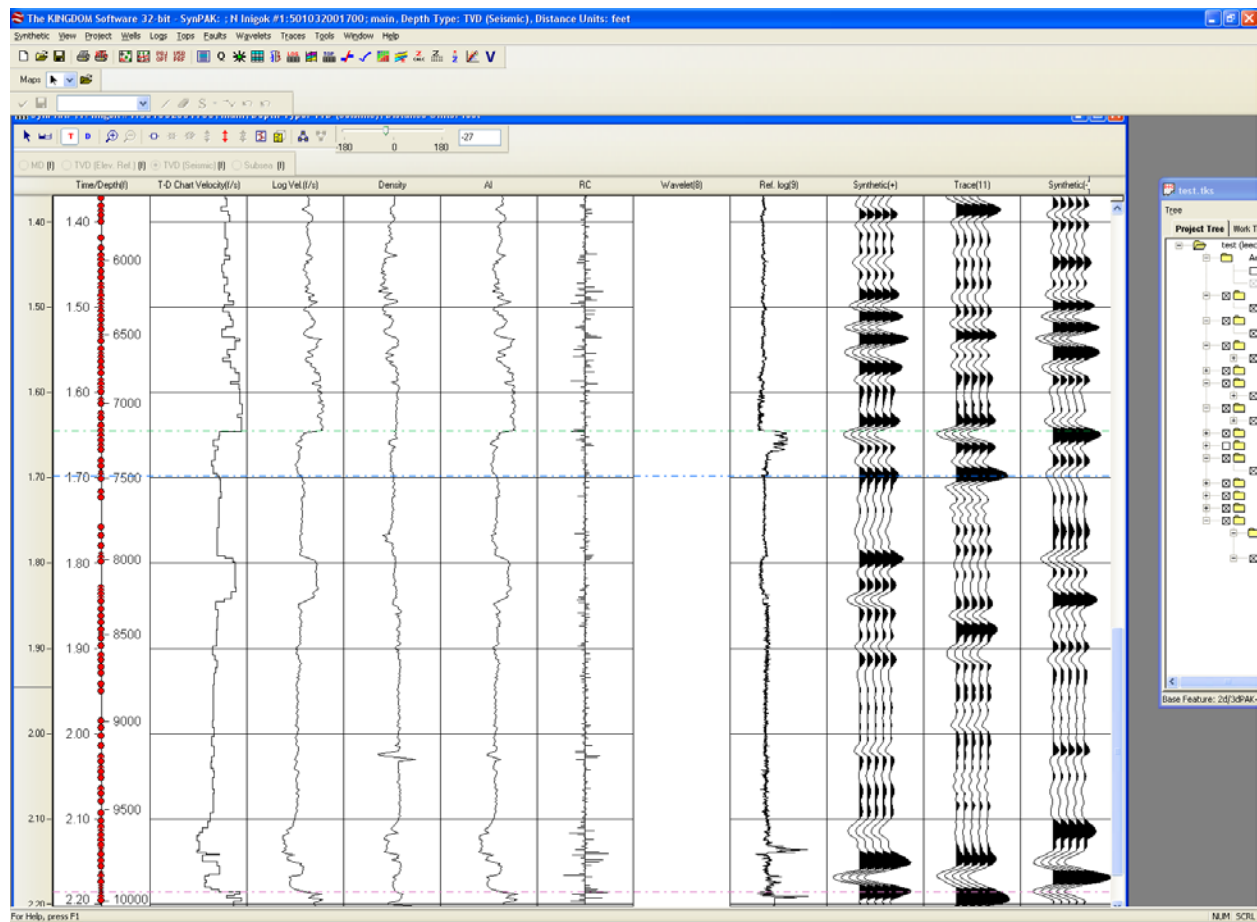
Screen Shot from KINGDOM© showing the petrophysical analysis within the Kingak along the Inigok well.



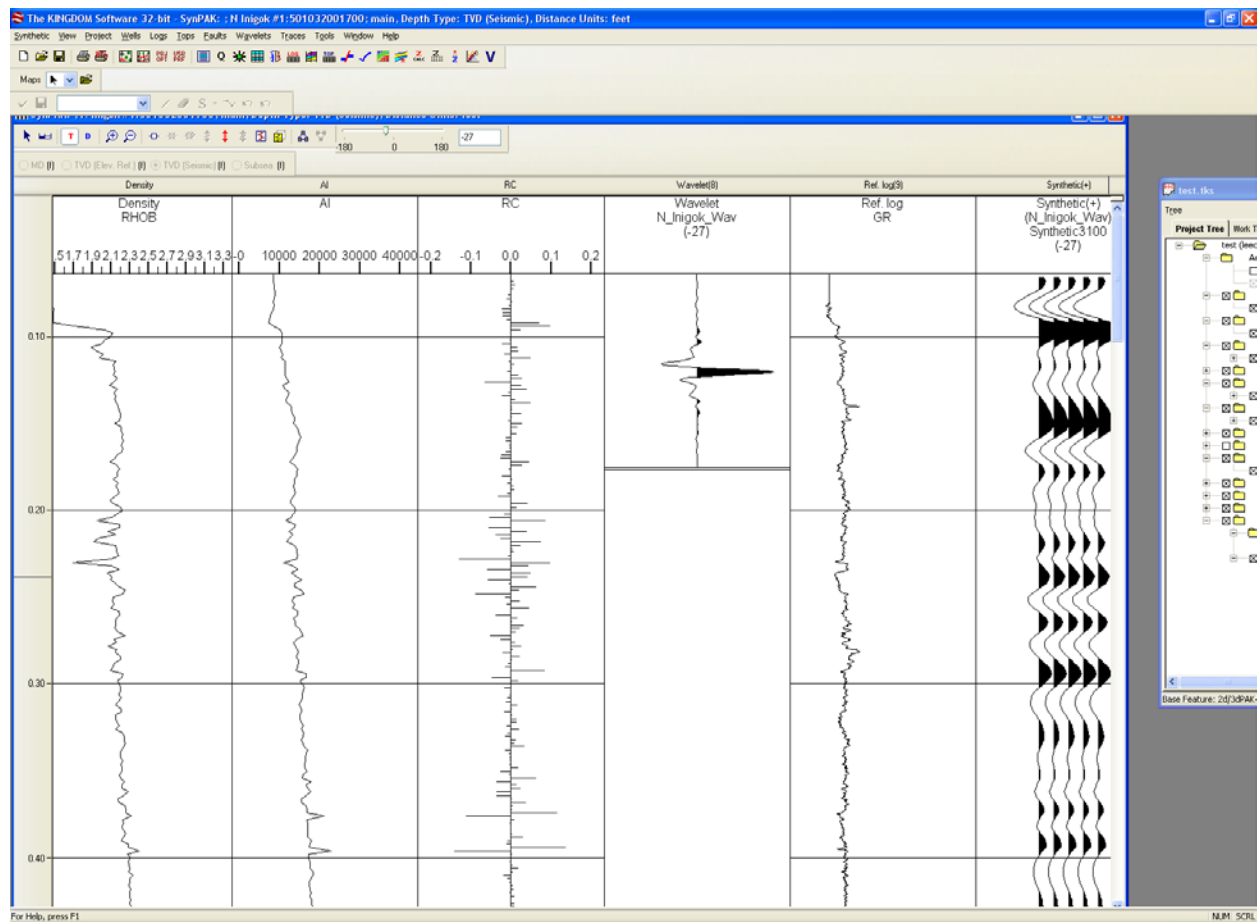
44



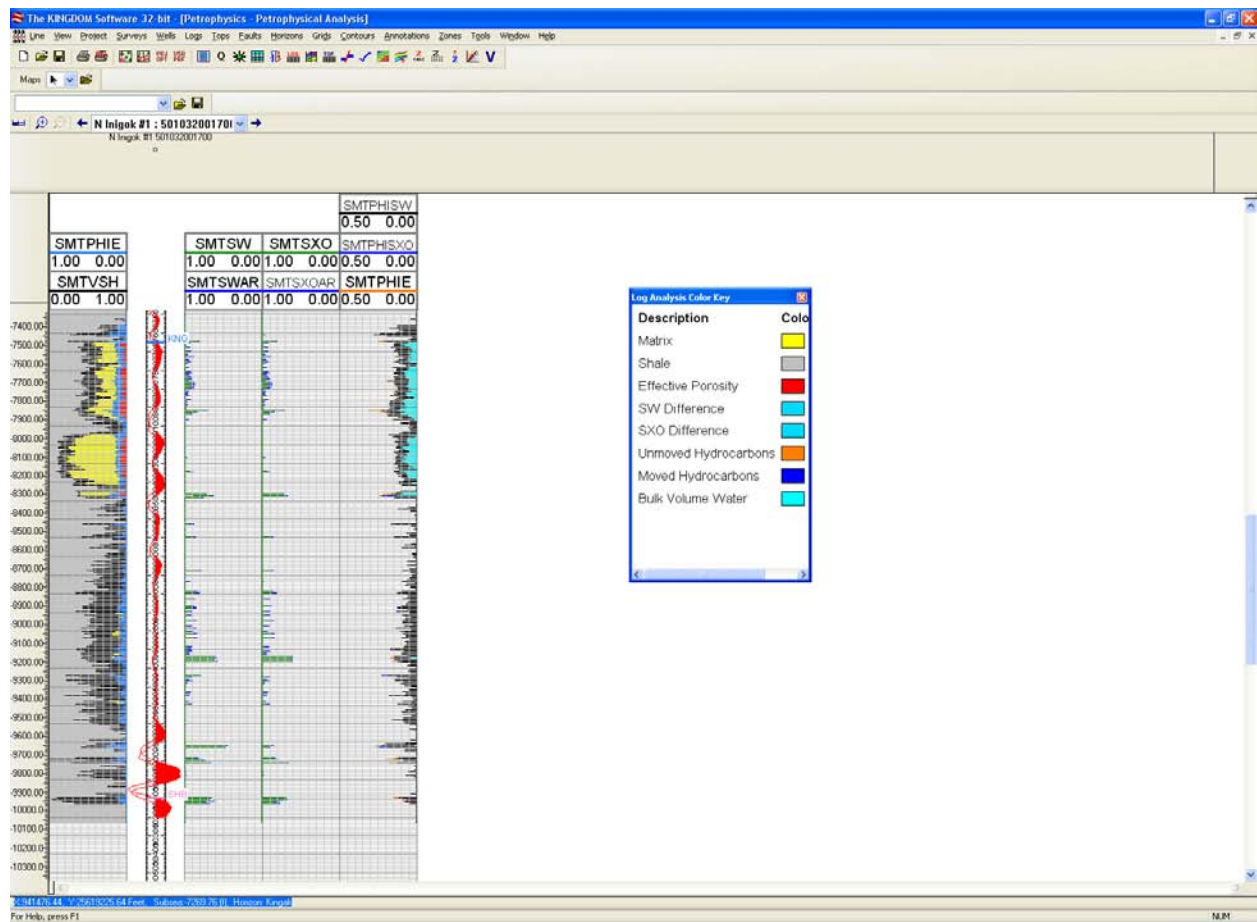
Screen Shot from KINGDOM© showing the top of the Synthetic Seismogram for the N Inigok well. The wavelet was rotated -27 for a best fit.



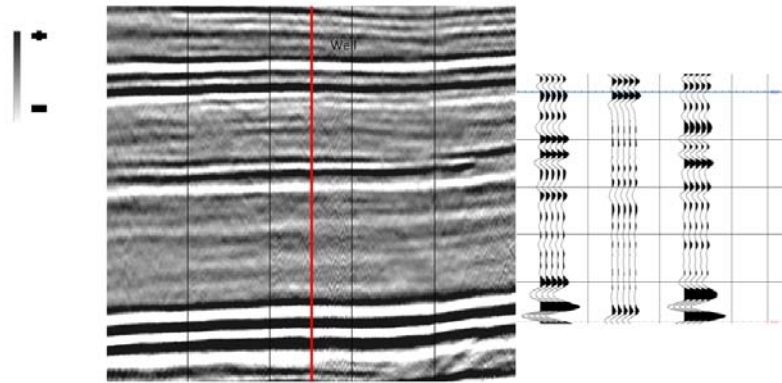
Screen Shot from KINGDOM© showing the bottom of the Synthetic Seismogram for the N Inigok well.



Screen Shot from KINGDOM© showing an enlargement of the Wavelet. The Wavelet was rotated -27 for a better fit.

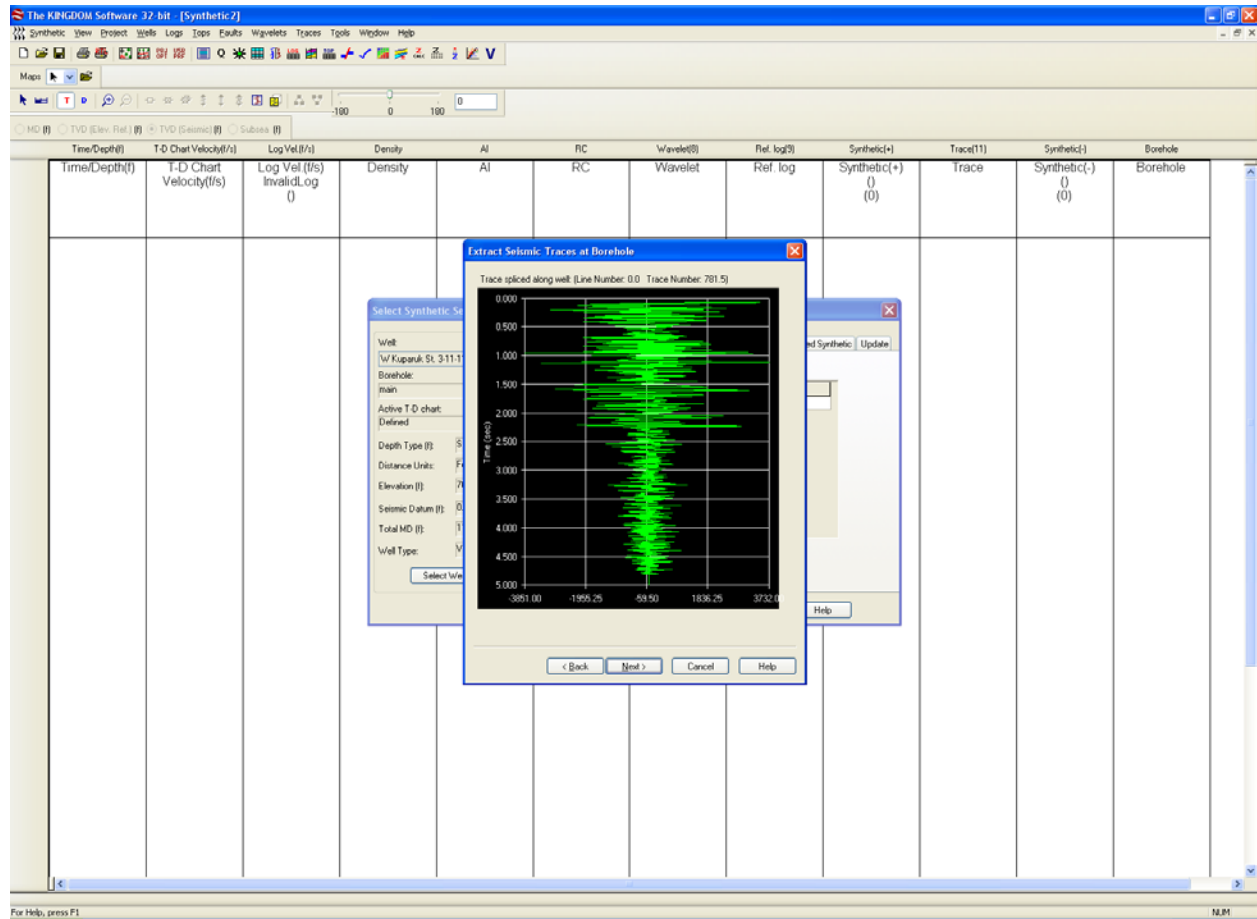


Screen Shot from KINGDOM© showing the petrophysical analysis within the Kingak along the N Inigok well.

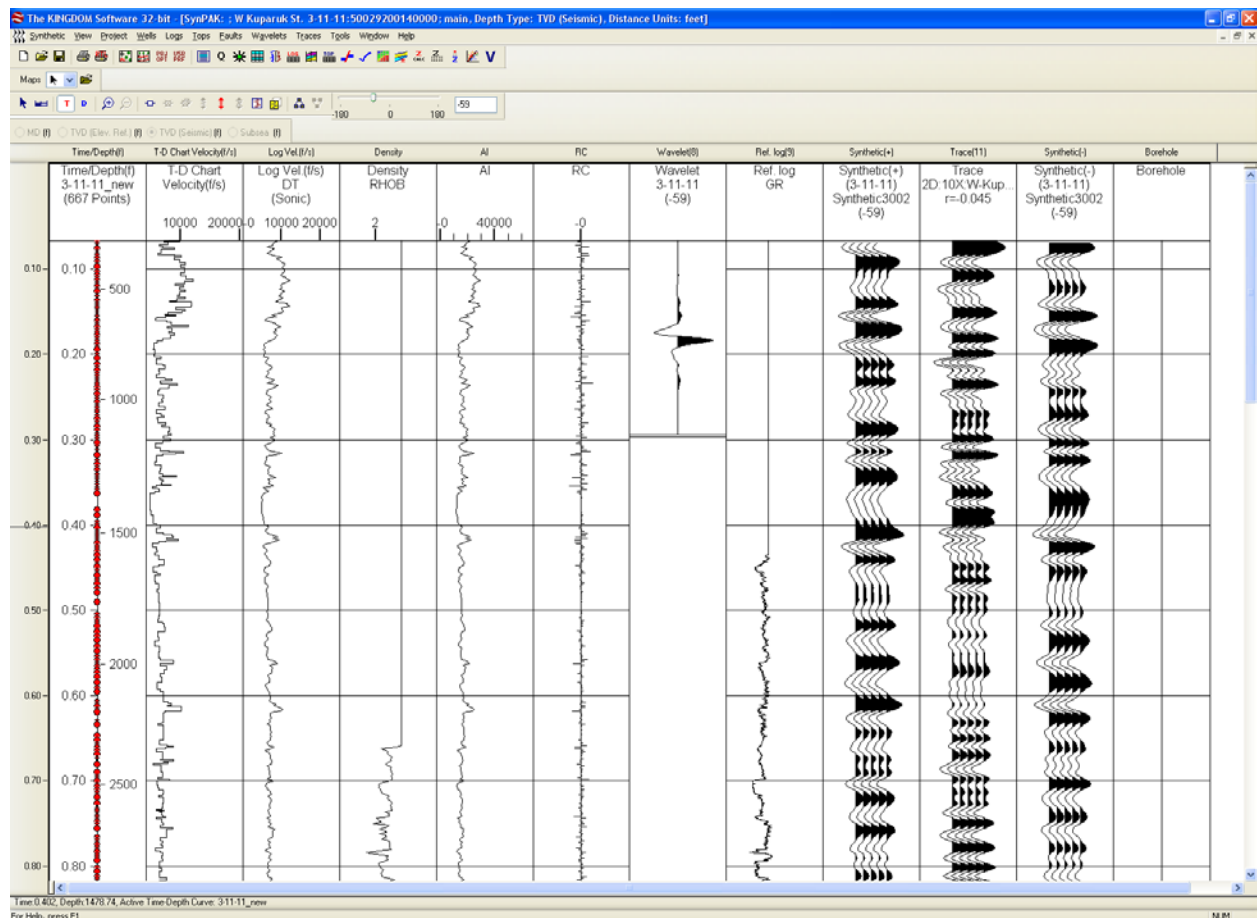


Seismic section showing the correlation between the seismic display and the Synthetic Seismogram along the N Inigok well.

## Appendix E: W Kuparuk

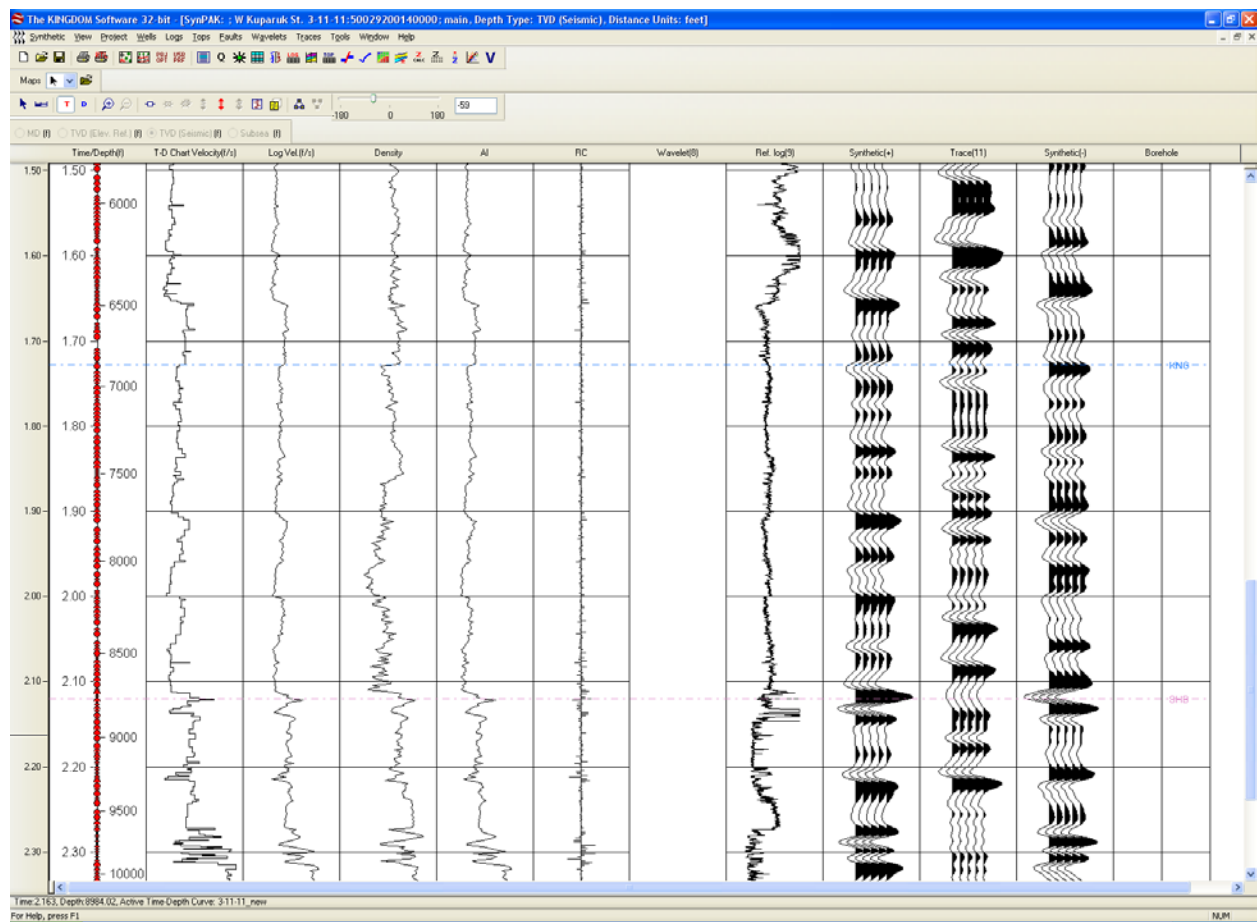


Screen Shot from KINGDOM© showing the extracted trace from along the borehole of the W Kuparuk well.

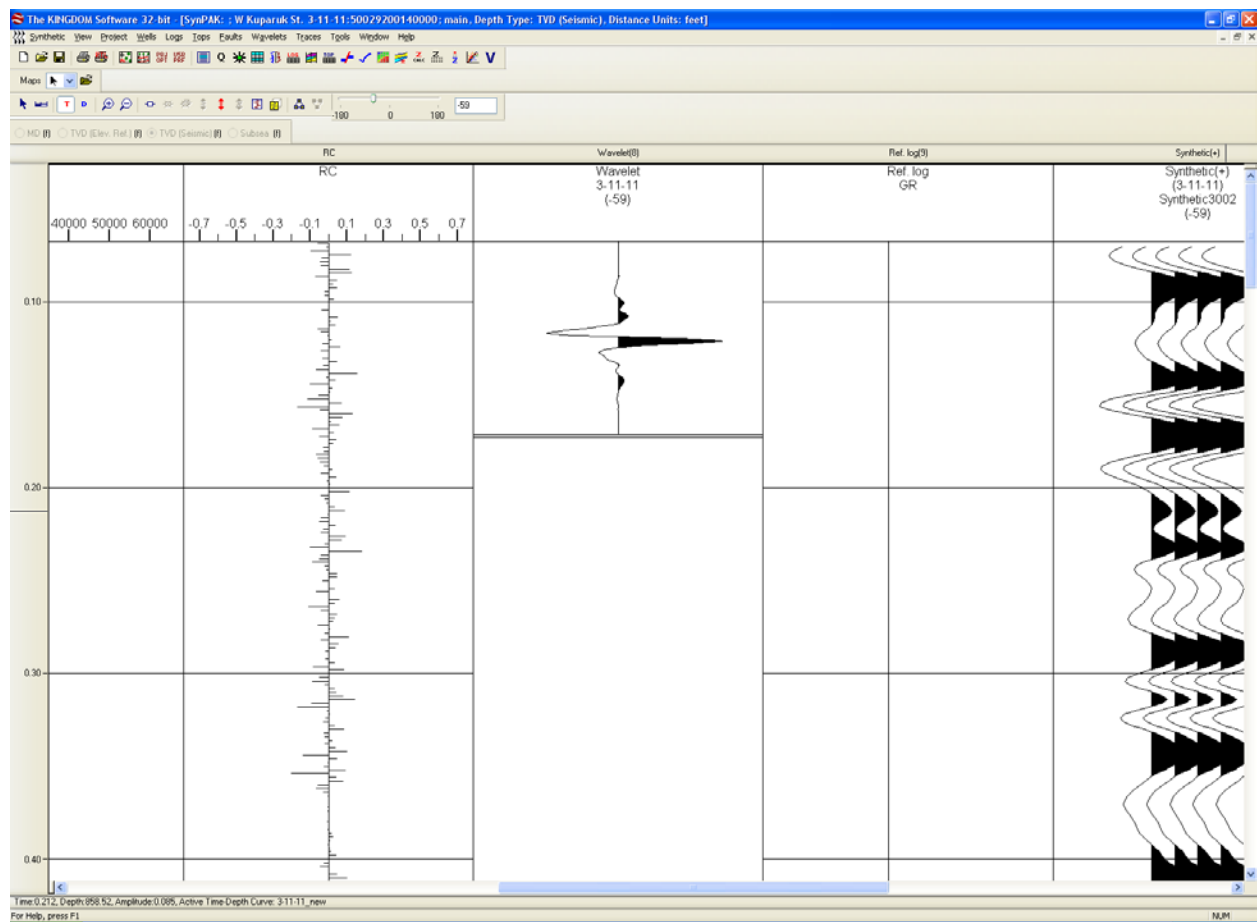


Screen Shot from KINGDOM© showing the top of the Synthetic Seismogram for the W Kuparuk well. The Wavelet was rotated -59 for a best fit.

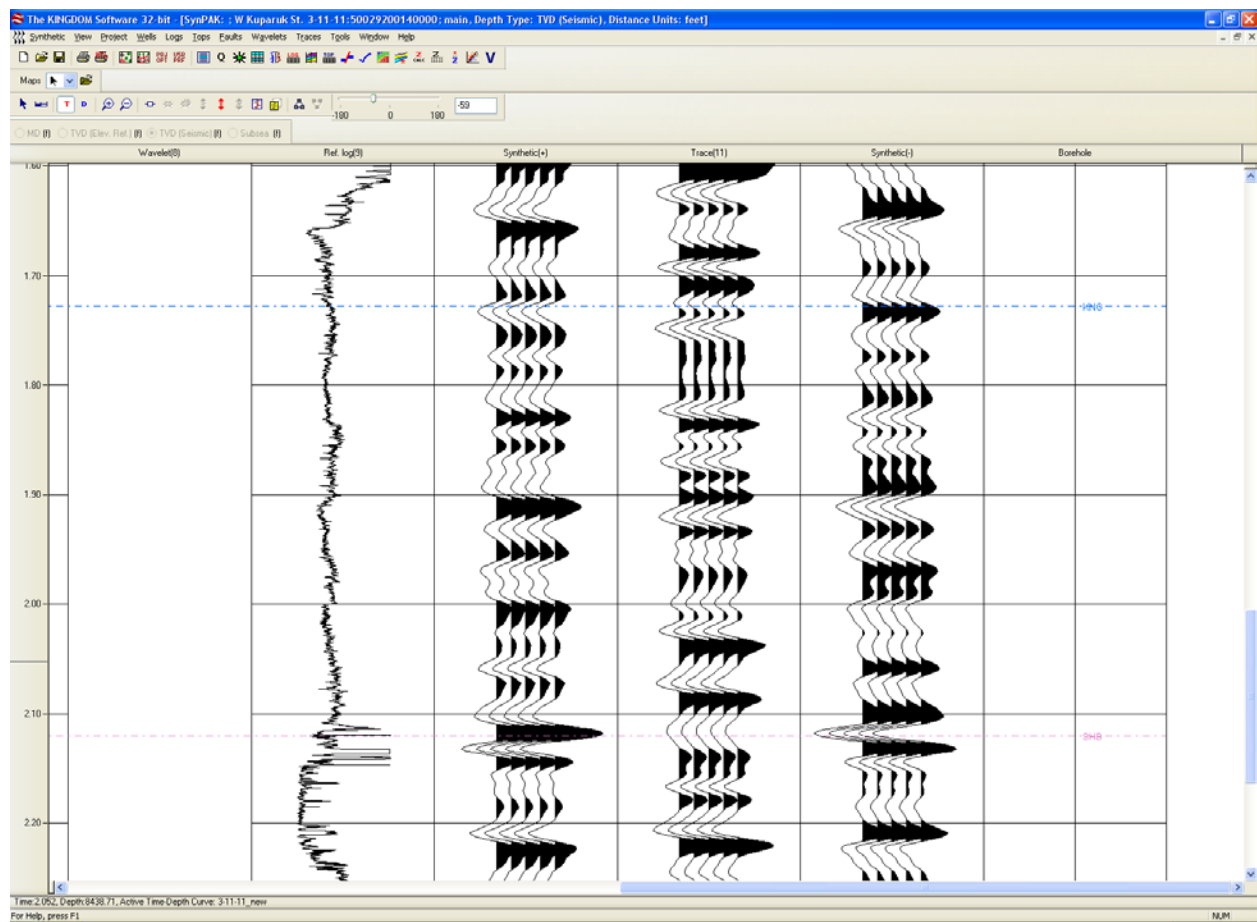




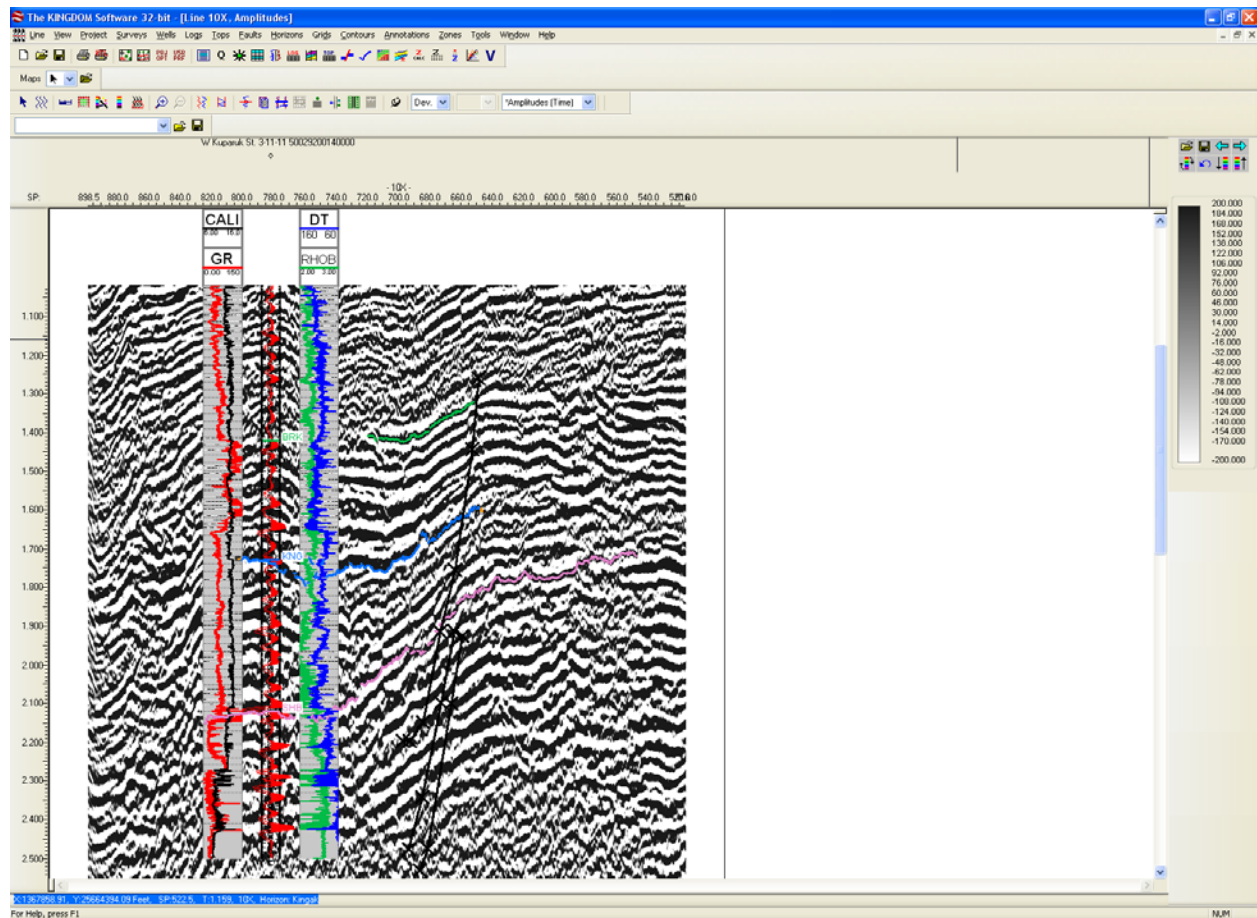
Screen Shot from KINGDOM© showing the bottom of the Synthetic Seismogram for the W Kuparuk well.



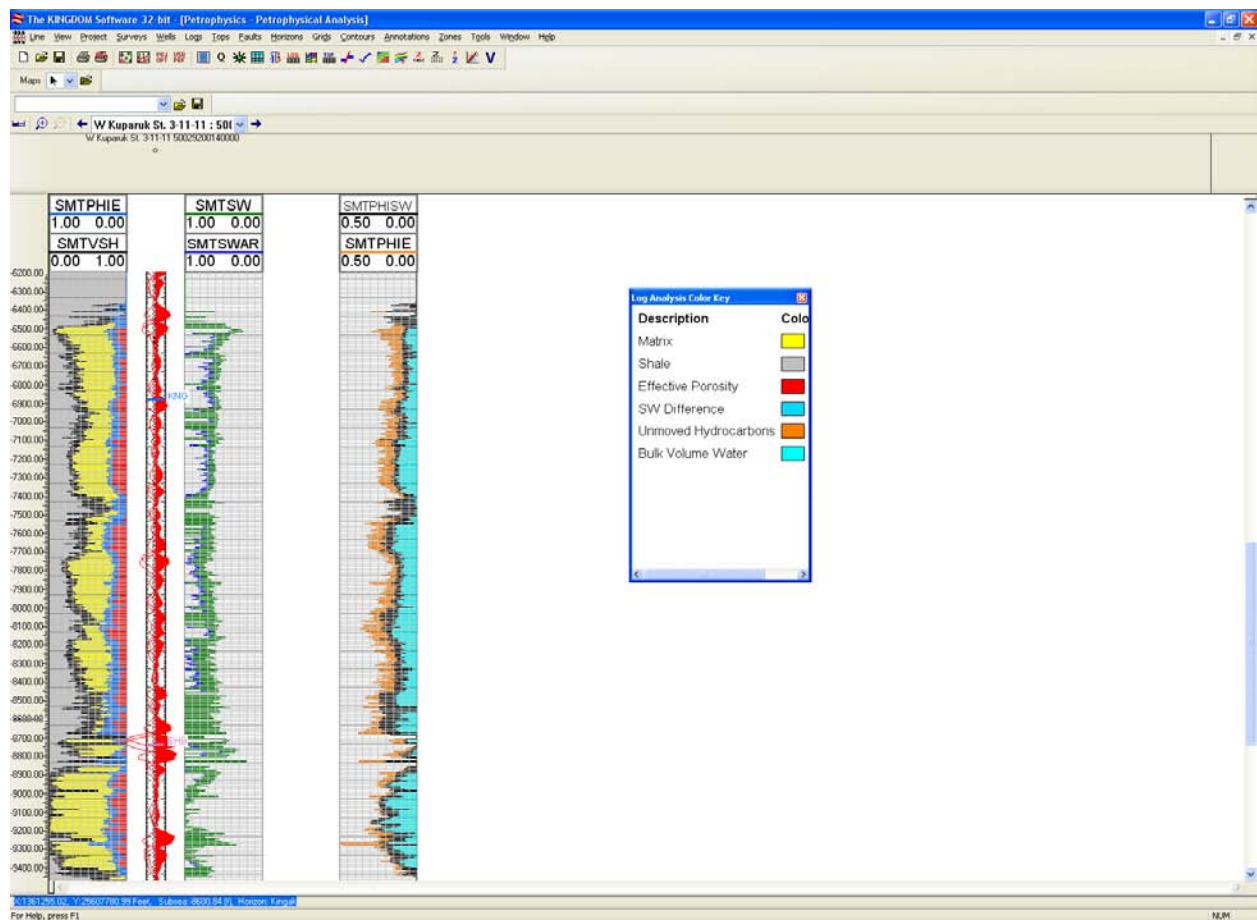
Screen Shot from KINGDOM© showing an enlargement of the Wavelet that has been rotated -59.



Screen Shot from KINGDOM© showing an enlargement of the Kingak section of the extracted trace and it correlation to the generated synthetic trace.



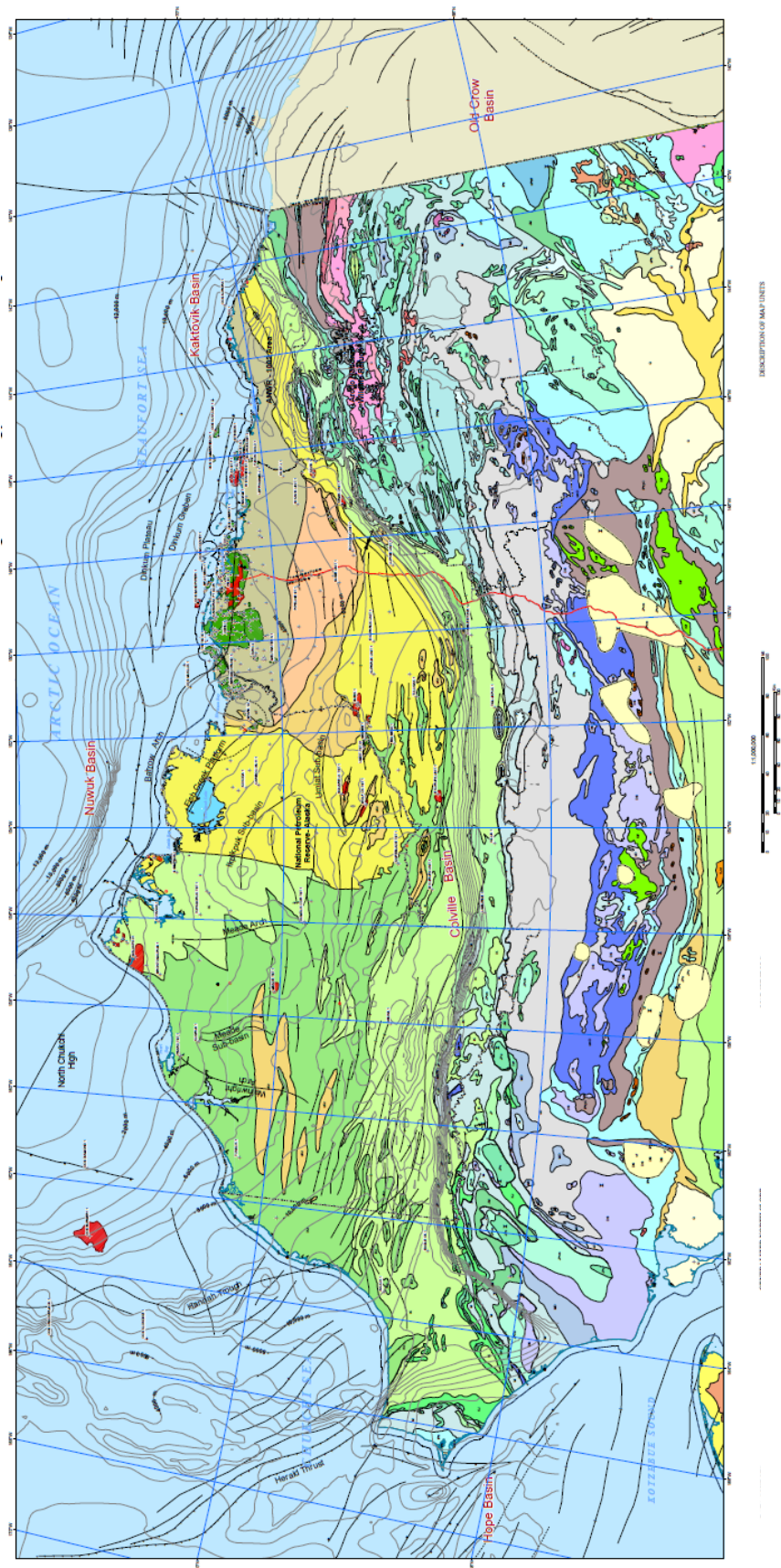
Screen Shot from KINGDOM© showing the seismic image along line 10X. The exact location of the well was unknown. Based on a visual estimation of its placement along the line 10X from Google Earth as well as matching the formation tops according to their known depths this seemed the most logical placement of the well. This study was unable to continue to the inversion stage, however, any future trials will need to ensure accurate placement of all wells.



Screen Shot from KINGDOM© showing the petrophysical analysis within the Kingak along the W Kupanuk well.

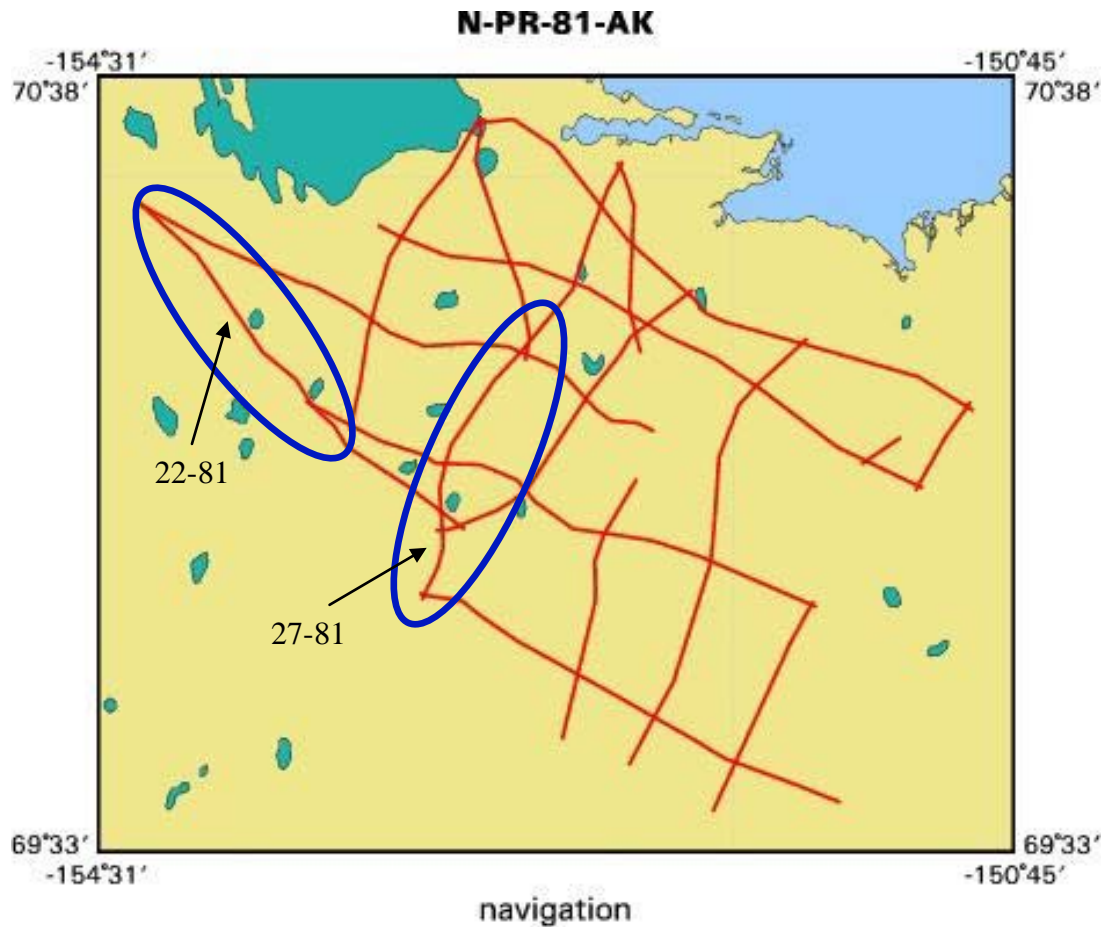


Appendix F: Structural Map North Slope



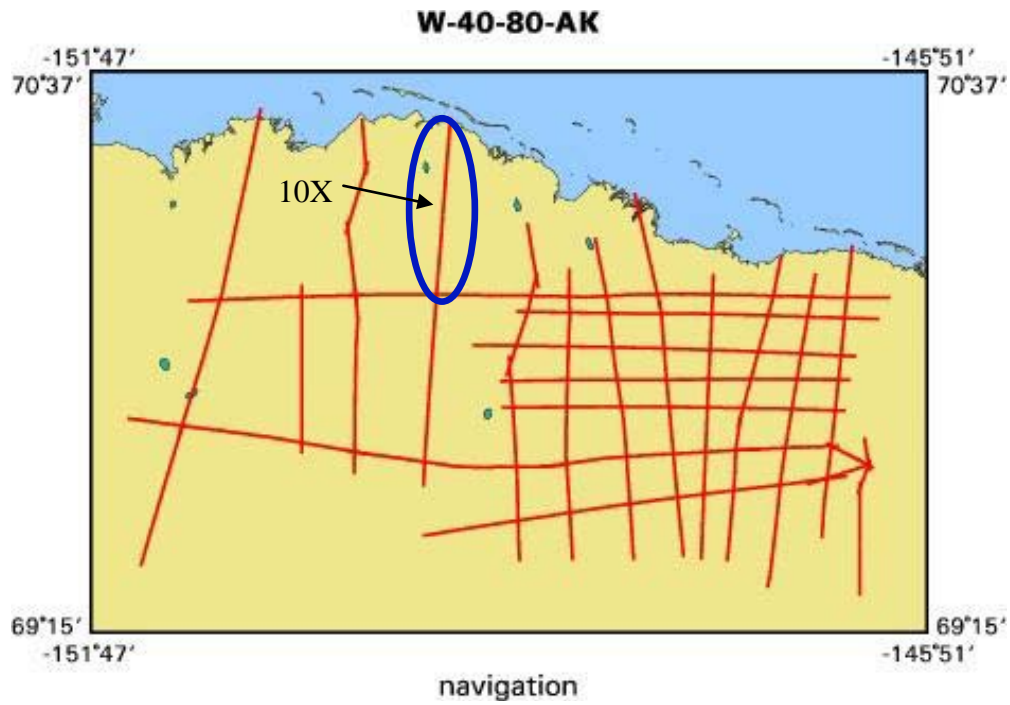
Appendix F: Structural map of the North Slope of Alaska. Modified from Mull et al., 1987

## Appendix G: Seismic data set N-PR-81-AK



Blue circles indicate seismic lines selected for study. Modified from *USGS*, 1974-1981

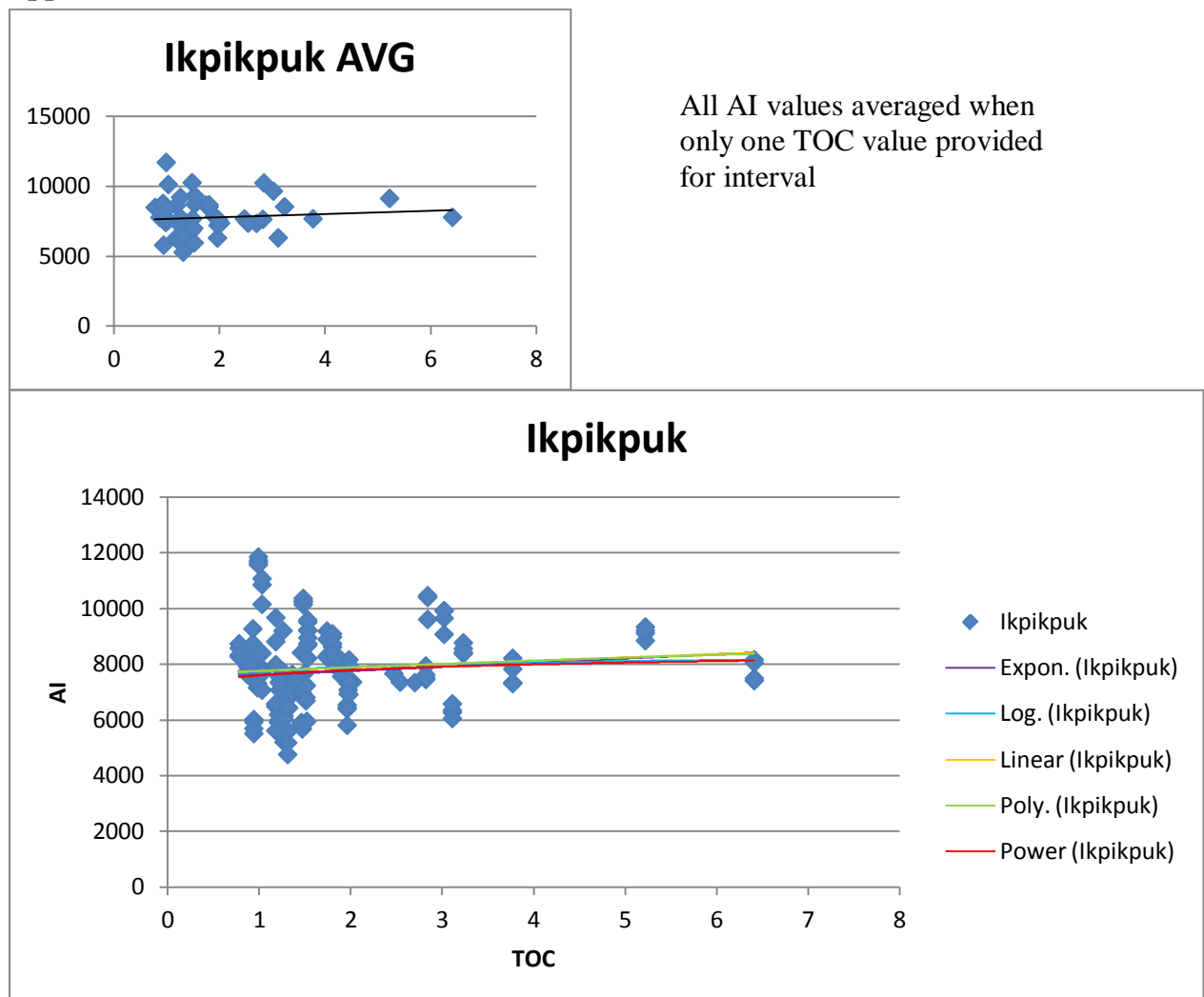
## Appendix H: Seismic data set W-40-80-AK



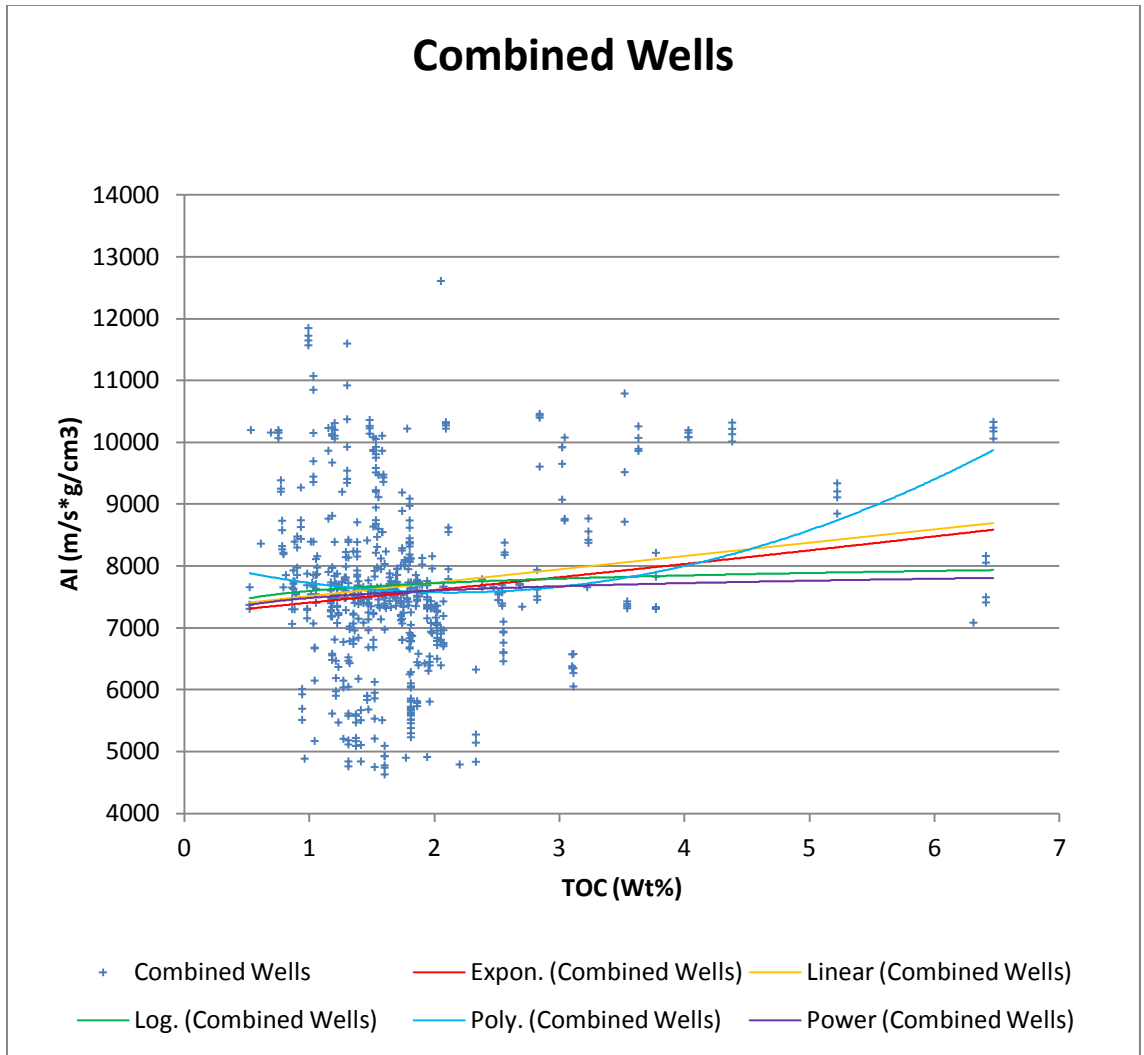
Blue circle indicates seismic line 10X selected for study. Modified from *USGS*, 1974-1981.



## Appendix I: Alternate Trend Lines

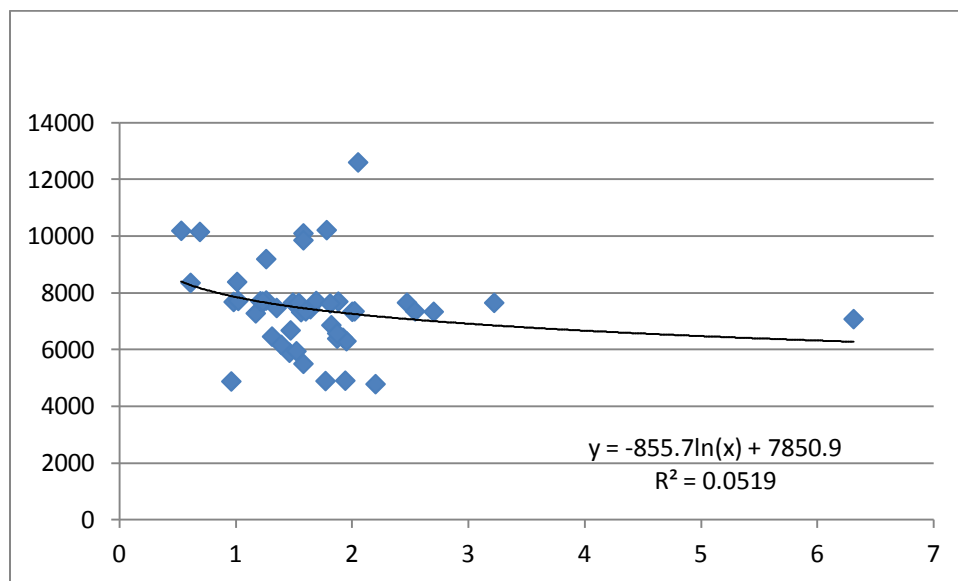


All possible trend lines applied to the Ikpikpuk data points.

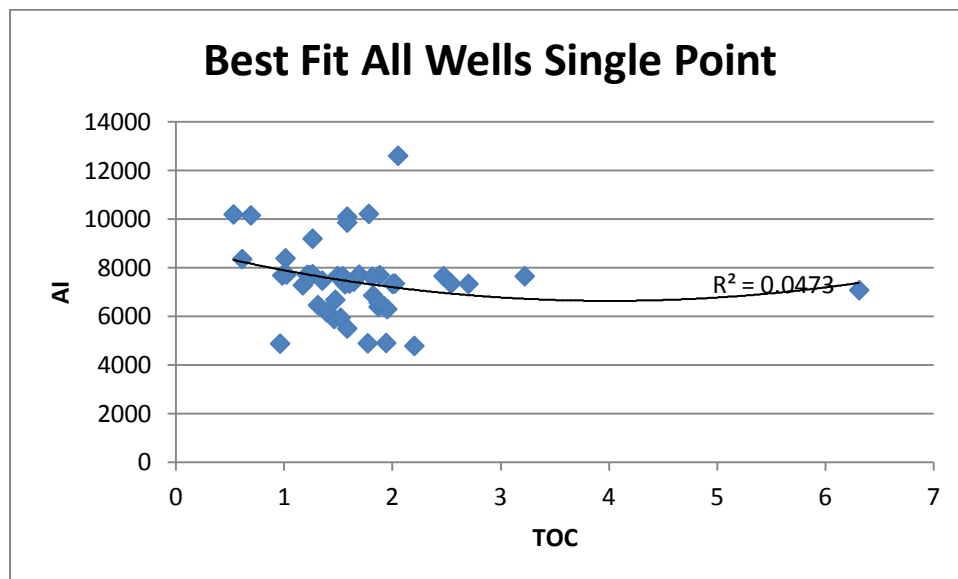


All possible trend lines applied to combined well plot.

## Appendix J: Alternate Plots Using Only Single Point Sources



Logarithmic Fit



Exponential Fit

**Vita**

Sarah Leedberg was awarded a B.A. in Geosciences from the University of Southern Maine. Prior to earning her bachelor's degree she received the Geological Society of America – Exxon Mobil Bighorn Basin Award.

Permanent address: 207 Bear Run Drive  
Pittsburgh, PA 15237

This thesis was typed by Sarah Leedberg

And was formatted by Teira Solis